HIGH-ENERGY INTERACTIONS BETWEEN ELECTRONS AND POSITRONS

V. N. BAĬER

Usp. Fiz. Nauk 78, 619-652 (December, 1962)

I. INTRODUCTION

QUANTUM electrodynamics, which is the most modern description of the interaction between charges and the electromagnetic field, was ultimately developed in the late Forties, when the renormalization theory was formulated. Measurement of the level shifts of atomic electrons, of the anomalous magnetic moment of the electron, and of many other effects has shown splendid agreement between theory and experiment. This success was attained, however, by systematic utilization of the method of subtracting the diverging integrals (renormalization), purely a cookbook procedure. Nonetheless, the situation in quantum electrodynamics is much more favorable than in theories of other interactions. In spite of the considerable progress in the theory of dispersion relations and spectral representations, some questions connected with the structure and quantitative description of strong interactions remain unclear. As regards the weak interactions, although the V-A variant of the theory is in good agreement at low energies with experience in the case of leptons, it is not clear whether this variant is applicable (and even the four-fermion interaction itself) at high energies. The theory was constructed without solving the main problem, namely the structure of space-time and the structure of the interactions at small distances, although ideas concerning the existence of a minimum limiting length were advanced many times. We set aside the fact that the theory does not enable us to calculate the masses, spins, and other characteristics of elementary particles.

Nonetheless, in spite of this shortcoming of the theory, not one of the hitherto performed experiments contradicts it directly. Were such a contradiction to be established, it would indicate the trend for further development in the theory, and it would seem that a contradiction must be sought at small distances.

Inasmuch as there is no quantitative theory of strong interactions, the discrepancy between experiment and modern theoretical notions can be established only if new qualitative regularities are discovered. A similar situation obtains for weak interactions, too. Matters are entirely different in the case of electromagnetic interactions, where there is a theory that is in splendid quantitative agreement with experiment, and any disparity between theory and experiment can lead to a radical review of our notions concerning the events that take place at small distances. This is precisely why electrodynamic experiments are the most promising method of investigating the limits of applicability of modern theory.

However, a specific formulation of electrodynamic experiment has been fraught until recently with appreciable difficulties; the point is that only classical electrodynamic objects, such as electrons and photons can be employed in such experiments, for the use of other particles (including muons) gives rise to unknown form factors in the theoretical formulas. If the experiments are performed on a target that is at rest, it must be recognized that the energy E_c in the center of mass system (c.m.s.) is connected with the energy in the laboratory system (l.s) E_l in the following manner:*

$$E_c = \frac{1}{2}\sqrt{2E_l m}, \qquad (1.1)$$

and E_l = 6000 MeV and E_c = 38 MeV for the maximum electron energy that can be hopefully obtained from accelerators in the conceivable future. (Data on accelerators now existing, under construction, and projected, for energies in excess of 1 Bev and for large currents, are listed in Table I.) Thus, the c.m.s. energy of electrons scattered by a target at rest is too small to allow us to speak, at the accuracies attainable at the present time, of a check on the applicability of quantum electrodynamics at small distances. Even now, the validity of quantum electrodynamics has been established for considerably smaller distances than can be measured in experiments wherein the c.m.s. electron energy is several times 10 MeV. This follows, for example, from experiments on the scattering of high-energy electrons by protons, measurements of the electron and muon anomalous magnetic moment, and many other experiments (this question is considered in greater detail in Chapt. III). An analogous situation arises also in the case of the scattering of photons by electrons of a target at rest.

The situation changed radically when the experimental feasibility of so-called colliding beams was demonstrated, in which two electron beams with equal but opposite momenta collide. In this case the experiment is carried out directly in the c.m.s. Experiments on the scattering of electrons in colliding beams are presently performed in many laboratories,

*We use the system of units where $\hbar = c = 1$ throughout.

Table I. High-energy or large-current electron accelerators both existing and projected

Accelerator	Maximum energy, BeV	No. of particles accelerated per second	Starting date	Remarks
1. Linear accelerator[9] of the Stanford University.	1.2	$3 \cdot 10^{12}$	1960	Placed in operation gradually, starting with 500 MeV in 1955
2. Cornell electron synchrotron[9] (Ithaca, New York).	1.5	10^{11}	1955	Operates at 1.2 BeV
3. California synchrotron[9] (Pasadena, California).	1,2	10^{9}	1956	
4. Electron synchrotron of the Frascati laboratory (Rome, Italy).	1.2	$6 \cdot 10^{10}$	1956	
5. Cambridge electron synchrotron (Cambridge, Mass.).	6.0	$6 \cdot 10^{12}$ project	1962	Already in operation
6. German electron synchrotron[9] (Hamburg).	6.0	$5 \cdot 10^{12}$ project	1963	
7. Linear accelerator[7] of the National Bureau of Standards (Washington, D. C.).	0.15	$3 \cdot 10^{15}$ project		Strong current
8. Electron synchrotron[9] (Tokyo, Japan).	1.2	$2 \cdot 10^{11}$	1961	
9. Stanford two-mile linear accelerator[9].	up to 45			Approved project

in particular with electron energy up to 500 MeV in each beam (corresponding to a laboratory-system energy of 10^{12} eV!). An experimental colliding-beam scheme is considered in Chapt. II.

The development of strong-current electron accelerators (see Table I) permits the conversion of electrons into positrons on much larger scales and to experiment with positron beams. Of exceptional interest is the creation of colliding electron-positron beams. We note that these beams can also be obtained when the intensity of the positron beam is relatively low; it is necessary to have in this case a storage ring with a long lifetime. These beams can be used not only to check the limits of applicability of quantum electrodynamics, but also to discover new charged-particle pairs and single neutral particles, to investigate the electromagnetic form factors of elementary particles, and to investigate the interactions between different elementary particles. These questions are considered in Chapt. IV.

Finally, experiments with colliding beams can also answer the question whether any weak interaction exists between electrons. This group of questions is considered in Chapt. V.

II. SCHEME OF EXPERIMENTS WITH COLLIDING BEAMS

Experiments with colliding beams aimed at studying the electron-electron scattering at high energies were proposed in 1956—1957 [1,2]. For the reasons pointed out above, these experiments attract presently much attention, and particularly, according to available data [3,4], experiments with colliding beams with electron energy of 500 MeV in each beam are being carried out presently at Stanford University. In many laboratories throughout the world experiments with colliding electron-positron beams are under preparation; in particular, at the National Laboratory in Frascati (Italy), an operating model of a suitable installation has been constructed to investigate the physical processes that occur during the course of storage of electrons and positrons; both electrons and positrons are obtained in this installation upon conversion of photons from an accelerator into an electron-positron pair [95,96].

Let us consider the principal installation scheme for experiments with colliding electron-electron beams. The electron beam 1 emerging from the accelerator (Fig. 1) is injected with the aid of a system of turning magnets and momentum inflectors (2 and 3) into two magnetic storage rings 6, and the electron radiation losses are compensated by an external electromagnetic field in resonators 4, while the beams circulating in the storage rings collide in the region 5; the electrons which are scattered at an angle of 180° are registered by high-speed counter pairs connected in a coincidence circuit 7.

Both storage rings act like synchrotrons. Upon injection, the momentum inflectors ensure the capture of the electrons into orbits. In compensating the radiation losses, the external field replenishes only the longitudinal component of the electron momentum, whereas the radiation carries away both longitudinal and transverse momentum. Consequently the electron clusters contract during storage. The planes in which

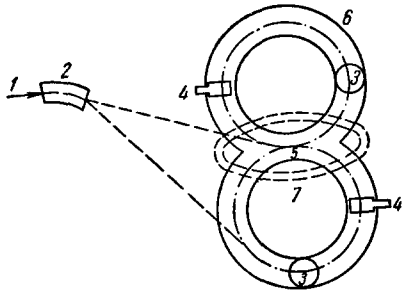

FIG. 1

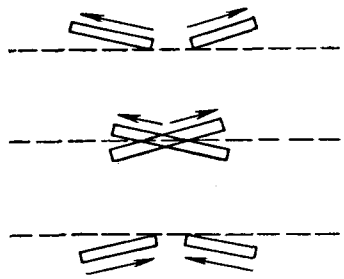

FIG. 2

the beams rotate can be slightly inclined to each other, so that the clusters cross in a small region (Fig. 2).

The colliding-beam experiment differs in principle from all the hitherto performed experiments where the scattering has been on stationary targets. The following new problems arise here: 1) the presence of the beams on the orbits for a time long enough to perform the experiment; 2) the time needed for a sufficient number of scattered electrons to be registered, in view of the low particle density in the "target." 3) the specific peculiarities involved in separation of the observed phenomenon from the background. Let us consider these questions briefly.

As a result of the relatively low particle density in the "target" (colliding beam) it is desirable that the beams exist on the orbits for a sufficiently long time. Whereas in accelerators the lifetime of the beam is determined essentially by multiple processes (multiple Coulomb scattering, quantum fluctuations in the radiation), the dominant role in the storage rings is assumed by single bremsstrahlung and single elastic scattering. This is connected with the fact that in accelerators the comparatively short acceleration time is usually much smaller than the lifetime with respect to single processes. Under these conditions, the decisive role in the particle losses is played by multiple processes, all the more because the acceleration cycle starts at a relatively low energy, when the multiple-scattering cross section is large, and the beam dimensions are comparable with the dimensions of the working region, with radiative damping absent. As a rule, the injection into the storage ring occurs at high energy, so that the radiative damping is effective during the entire lifetime of the beam and the beam dimensions very rapidly drop below the permissible stability-region dimensions. Therefore the time during which the beam is contained in the storage ring is determined by single processes which change the characteristics of the particle radically. Emission of a bremsstrahlung quantum of relatively high energy upon collision of the electron with the nucleus of the atom of the residual gas in the storage ring chamber causes the particle to drop out of the stability region for longitudinal motion, so that the particle no longer receives energy to compensate for the radiative losses, and the orbit radius decreases until the particle strikes the chamber wall. In single Coulomb scattering through large angles, the particle is lost as a result of collision with the chamber wall. It is clear that the lifetime of the beam relative to each of these effects is inversely proportional to the density of the residual-gas atoms. If a high vacuum ($p \sim 10^{-9}$ mm Hg) is maintained in the chamber, then the aforementioned lifetimes amount to many hours. The influence of quantum fluctuations in radiation can be made sufficiently small, if the horizontal dimensions of the chamber are large (the quantum fluctuations lead to a horizontal broadening of the beam) and accelerating field of high intensity is applied.*

Let us proceed now to the following question: how fast can a set of readings of sufficient statistical size be accumulated? The electrons moving in the storage rings are gathered into clusters of length l. The diagram showing the collision between these clusters at the point of beam encounter is shown in Fig. 2. The number of electrons scattered per second in a solid angle $d\Omega$ can be represented in the form

$$dN = \frac{2N_1N_2f}{sq}\frac{l_{\text{int}}}{l}\sigma(\vartheta)\,d\Omega; \qquad (2.1)$$

where N_1, N_2—number of electrons in each beam, f—frequency of cluster revolution in the storage ring, $\sigma(\vartheta)$—electron-electron scattering cross section, s—transverse area of the cluster, q—number of harmonic of the accelerating voltage (number of clusters per orbit in each of the storage rings), l_{int}—dimension of the interaction region; the factor 2 is the result of the target motion.

Figure 3 shows the crossing of the beams in the interaction region. Assume that identical and homogeneous beams of height h and width d cross at an angle α. In practice the following case is realized: $\alpha \ll 1$ ($h/\sin\alpha \ll l$), and then

$$dN = \left(\frac{I}{e}\right)^2\frac{2\sigma(\vartheta)}{ldf\alpha}\,d\Omega; \qquad (2.2)$$

*A careful investigation of the lifetime of the beam in the storage ring has been recently made in [5,6] (see also [97]).

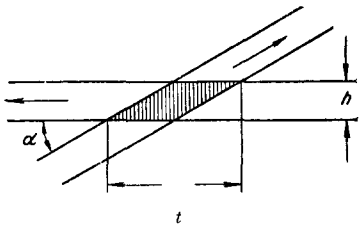

FIG. 3

Here I is the current that circulates in one of the tracks and e the electron charge. We see that in this situation the number of scattered electrons does not depend on the height of the clusters. If we assume $\alpha = 0.03$, $l = 20$ cm, d = 1 cm, and I = 1 A (at an orbit radius r = 1 meter this corresponds to 1.3×10^{11} particles in the cluster), then

$$dN = 3 \cdot 10^{30} \sigma(\vartheta)\, d\Omega. \qquad (2.3)$$

Inasmuch as the measured cross sections (see Chapters III and IV below) lie in the range 10^{-30}—10^{-34} cm^2/sr, it is clear that even a current of 1 amp yields fair statistics, if we take into account the fact that the beams can exist on the orbits for many hours.

Let us consider now the separation of the observed phenomenon from the background. We note first that the scattered electrons coincide exactly in time and move in almost exactly opposite directions; the radiation accompanying the scattering causes the scattering angle of the electrons to possibly differ from 180° (for more details see Chapt. III). Second, the scattered electrons have the same energy as the initial ones (disregarding the radiation losses), whereas the electrons scattered by a stationary target, for example by the nucleus of a residual-gas atom, lose appreciable energy to recoil or to inelastic processes. Any characteristic can be used to separate the investigated process.

Inasmuch as it is difficult to create instruments that subtend large solid angles and have high energy resolution, the principal means used to identify electron-electron scattering events presently is the indicated time and space correlation. An experimental setup intended to extract the electron-electron scattering events consists of many pairs of counters, distributed over the surface of a sphere surrounding the interaction region, and connected in coincidence with a resolution time $\sim 10^{-8}$—10^{-9} sec. The large number of counters is used to increase the effective solid angle of observation so as to accelerate the accumulation of the statistics, particularly in large-angle scattering. The background produced by the scattering of the electrons by the residual gas atom, by pion production on the residual gas, and also by cosmic rays is excluded quite satisfactorily by the coincidence circuitry.

Thus, the investigation of electron-electron scattering by the colliding-beam technique is perfectly feasible experimentally and can be carried out with high precision.

Of exceptional scientific interest is the creation of colliding electron-positron beams, which can be used not only to investigate the limits of applicability of quantum electrodynamics, but also for many other physical researches (see Chapters III—V). The fundamental new problem, on top of those listed above, is in this case the creation of a positron beam of high intensity (10^{11}—10^{10} particles in the beam)*. The conversion coefficient† μ of electrons with energy E_0 into positrons with energy E_+ in an energy interval dE_+ has been calculated for practical converter thicknesses in [8]; for example, for $E_0 = 500$ MeV, $E_+ = 250$ MeV, and $dE_+/E_+ = 5$ per cent we get $\mu = 1/400$ if the convertor thickness is approximately equal to the radiation length unit. The created positrons are emitted essentially forward; in the example considered, rough estimates show that the angular spread of the positron beam is ~4°. Thus, other conditions being equal, to produce a positron beam the required electron beam must have some one-thousand times more intensity than is necessary to produce colliding electron-electron beams. On the other hand, if the positron beam is obtained by storage in small batches, the storage time is accordingly increased by a thousand times.

In addition, the separation of the observed phenomenon from the background becomes a much more complicated matter. This is connected with the fact that elastic electron-positron scattering is accompanied here by two-quantum annihilation, and by production of pairs of charged particles, with the probabilities of all these processes approximately equal. It is clear that each of these processes will produce paired coincidences. However, inasmuch as each of these processes is of great physical interest, the problem consists in fact not of cutting out the background but of separating (and possibly simultaneously observing) the different processes. Modern experimental means are perfectly capable of coping with such separation.

A possible scheme for obtaining colliding electron-positron beams is shown in Fig. 4. Inasmuch as the electrons and positrons rotate in the magnetic field in opposite directions, one storage ring is used in this case. The electron beam from accelerator 1 enters into converter 2, from which the emerging positron beam is focused and brought by means of

*We note that positron annihilation in flight does not influence the beam lifetime. Indeed, the annihilation cross section is much smaller than the elastic electron-electron scattering cross section, and this scattering does not influence practically the lifetime of the beam in the electron storage ring.

†The conversion coefficient μ is defined as

$$\mu = \frac{\text{number of positrons with energy } E_+ \text{ in interval } dE_+}{\text{total number of initial electrons}}$$

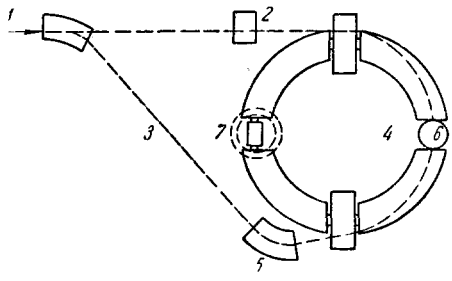

FIG. 4

inflector 6 into storage ring 4; conversion is accompanied by energy loss (in the case considered here the energy is reduced to one-half). The storage ring operates like a synchrotron, and after a sufficient number of positrons is accumulated in it it changes to an accelerator mode, raising the positron energy to the value of the incident electron beam energy. The electron beam is then guided directly to the storage ring from the accelerator 3 by means of the system of deflecting magnets 5 and the inflector 6. In such an injection system it may be advisable to use electron and positron beams of different intensity, say a circulating electron current I_e = 10 A and a circulating positron current I_p = 0.1 A, although the accelerating-field generator must in this case have a higher power than in the case of equal currents in order to obtain a given number of counts. If we assume that the beams have identical dimensions, then the number of particles scattered (or created) in a solid angle $d\Omega$ will be

$$dN = \frac{I_e I_p}{e^2} \frac{2\sigma(\vartheta)}{ldfa} d\Omega; \qquad (2.4)$$

Here $\sigma(\vartheta)$ is the differential cross section of the process of interest to us. Thus, to guarantee a sufficient rate of accumulation of statistics we can use currents of 10 A and 0.1 A in place of two currents with intensity 1 A.

The lifetime of electron and positron clusters captured in the storage ring were measured in the storage ring model for electron-positron colliding beams in the Frascati (Italy) laboratory, in which processes connected with storing are investigated. The experiments carried out with clusters of negligible intensity have shown that in a vacuum of 4×10^{-10} mm Hg the beam lifetimes reach 48 hours.

The scattered (created) particles are registered in the case of two-particle processes by pairs of counters connected in coincidence and distributed over the surface of a sphere surrounding the point of encounter 7.

Naturally, to produce colliding electron-positron beams it is desirable to have strong-current electron accelerators, such as accelerator No. 7 of Table I, where monoenergetic electron beams with intensity $\sim 10^{11}$ particles/second are expected to be produced.

Let us make, finally, one remark concerning types of storage rings. We have seen that the number of scattered (created) particles increases with decreasing cross section of the cluster. In storage rings with hard focusing, the cross section of the cluster can be made approximately 100 times smaller than in storage rings with weak focusing. It is particularly important to use this margin at very high energies (above 1 Bev), where the cross sections of the processes decrease rapidly, all the more since in storage rings with hard focusing the requirements imposed on the intensity of the accelerating field are less stringent. These requrements are quite burdensome in the case of high energy in view of the fast growth (proportional to the fourth power of the energy) in the radiation losses.

III. CHECK ON THE APPLICABILITY OF QUANTUM ELECTRODYNAMICS AT SMALL DISTANCES

3.1. Calculation of the radiative corrections to electrodynamic cross sections. Experiments on the scattering of electrons in colliding beams are proposed for a check on the applicability of quantum electrodynamics at small distances. As was already noted, in view of the fact that quantum electrodynamics is a quantitative theory, any deviations of the experimental cross sections from the theoretically calculated ones will be evidence of failure of quantum electrodynamics at small distances. This is the undisputed advantage of such experiments over experiments in which strongly-interacting particles participate. In light of this, it is of particular importance to take a correct account of all the theoretical contributions to the electrodynamic cross sections.

In the lowest perturbation-theory order, electron-electron scattering is represented by two Feynman diagrams (Fig. 5). The scattering cross section in this order was first calculated by Moller (see, for example [10,11])

$$\sigma_0(\vartheta) = \frac{r_0^2}{8\gamma^2}\left[\frac{s^4+q'^4}{q^4} + \frac{2s^4}{q^2q'^2} + \frac{s^4+q^4}{q'^4}\right]; \qquad (3.1)$$

Here r_0 is the classical radius of the electron, $\gamma = E/m$, E is the energy of the electron, $s = p_1 + p_2$, $q = p_1 - p_1'$, $q' = p_1 - p_2'$. The invariant variables s,

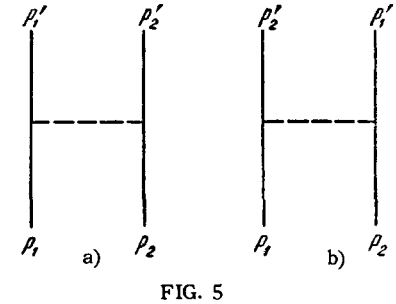

FIG. 5

q, and q′ will be used extensively from now on. In the c.m.s.*

$$q^2 = -2p^2(1-\cos\vartheta);\quad q'^2 = -2p^2(1+\cos\vartheta);\quad s^2 = 4E^2, \tag{3.2}$$

where ϑ is the scattering angle.

For ultrarelativistic electrons, Moller's formula can be reduced in the c.m.s. to the following simple form

$$\sigma_0(\vartheta) = \frac{r_0^2}{\gamma^2}\left[\frac{2}{\sin^2\vartheta} - \frac{1}{2}\right]^2. \tag{3.3}$$

To estimate the accuracy of this formula it is necessary to calculate the next higher terms of the perturbation-theory series in the coupling constant e, that is, to find the radiative corrections. Calculation of the radiative corrections of order e^6 was made in [12-19]. In this case it is necessary to consider the diagram shown in Fig. 6, adding to it the exchange diagrams ($p_1' \longleftrightarrow p_2'$). Figure 6 does not show graphs containing the self-energy of the electron, for these drop out in the regularization, which is carried out by standard means [10,11]. The matrix elements of diagrams 2, 3, 5, and 5′ diverge also in integration in the region of small virtual-photon momenta ("infrared catastrophe"). As is well known, the reason for it is that the very concept of an elastic process is purely arbitrary, for in each scattering event soft quanta are emitted, and the radiation cross section also diverges in the region of small frequencies, but the total cross section of elastic and inelastic scattering contains no divergences. Thus, to eliminate the infrared catastrophe it is necessary to take into account diagrams with emission of real photons (Fig. 7, to which the exchange diagrams must also be added).

An account of the emission of real photons greatly complicates the investigation of the scattering, since the cross section depends on the specific experimental conditions. In the early investigations [12,13] the calculation of the radiative corrections was made in the laboratory system, it being assumed that the soft quanta can be emitted in arbitrary directions ("isotropically") and that the total energy of the emitted quanta is $\Delta E \ll m$.

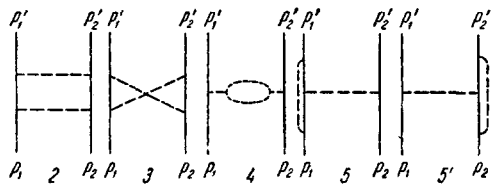

FIG. 6

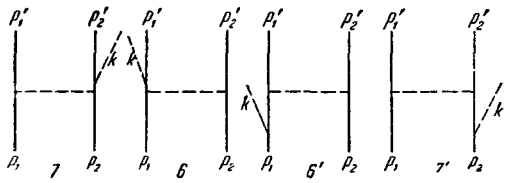

FIG. 7

The results of these calculations cannot be used directly to consider experiments with colliding beams since, first, the experiments are carried out in the c.m.s., and, second, the photons can, generally speaking, carry away an energy on the order of the initial electron energy. In fact, as we have already noted in Chapt. II, the scattered electrons are registered by counter pairs (Fig. 8) connected for coincidence. Inasmuch as the energy threshold of the counters is must smaller than the initial electron energy, the counters will register practically all the electrons that enter in them, independently of the energy lost by them. Thirdly, the emission of hard quanta upon scattering will be far from isotropic. To verify this, let us note that when the following conditions are satisfied [20]

$$\frac{e^2}{\pi}\ln\frac{m}{\Delta E}\ln\frac{E}{m} \ll 1 \tag{3.4}$$

the emission of quanta can be considered by perturbation theory. Inasmuch as in the energy region investigated at the present time we certainly have

$$\frac{e^2}{\pi}\ln\frac{E}{m} \ll 1, \tag{3.5}$$

investigation of the emission of real quanta with energy $\Delta E \sim m$ and higher can without a doubt be treated by perturbation theory. It follows from this therefore that if many quanta are emitted upon collision of the electrons, only one of these quanta will be hard, since the emission of two hard quanta occurs in the higher order of perturbation theory and has consequently low probability. The matrix element of diagrams 6 and 6′ can be represented in the form

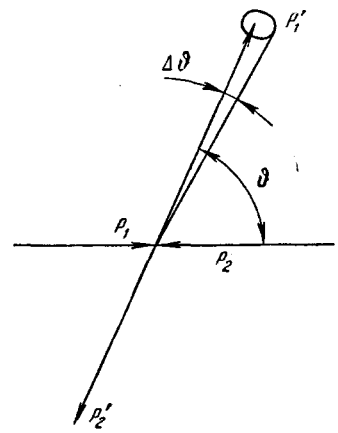

FIG. 8

*Here and throughout (ab) = $a^0b^0 - (\mathbf{a}\cdot\mathbf{b})$.

$$M_{6+6'}=\frac{e^3}{(2\pi)^{7/2}}\frac{m^2}{(2\omega E_1E_2E_1'E_2')^{1/2}}\frac{\bar u(p_2')\gamma^\mu u(p_2)}{(p_2'-p_2)^2}\bar u(p_1')\left[\left(\frac{(ep_1')}{(kp_1')}-\frac{(ep_1)}{(kp_1)}\right)\gamma_\mu+\frac{1}{2}\left(\frac{\hat e\hat k\gamma_\mu}{(kp_1')}+\frac{\gamma_\mu\hat k\hat e}{(kp_1)}\right)\right]u(p_1). \quad (3.6)$$

The matrix element of diagram 7 and 7′ has an analogous form, except that the denominators contain the combinations (kp_2') and (kp_2). Expressing the scalar products in terms of the angle between the momenta of the corresponding electron and photon, and in terms of their energy, we obtain

$$(p_ik)=\omega E_i(1-\beta_i\cos\vartheta_i), \quad (3.7)$$

where β_i is the electron velocity. Thus, in the expression for the photon-emission probability there appear characteristic denominators of the type (3.7). This causes the photons to be emitted ($\beta_i \to 1$) predominately in narrow cones about the directions of the initial and final electrons.

The photons emitted in inelastic electron collision can be arbitrarily subdivided into two classes—soft and hard. This division is closely linked with the geometry of the experiment. Let us assume that one of the scattered electrons has struck the center of one of the counters, and then the photon will be classified as soft if the second electron strikes the opposite counter, regardless of the photon emission direction. In the opposite case we shall assume that the photon is hard.

The maximum energy of the soft photons emitted in the cones around the directions p_1 and p_2 is

$$\varepsilon=\frac{E\Delta\vartheta}{\sin\vartheta+\Delta\vartheta\left(\frac{1+\cos\vartheta}{2}\right)}. \quad (3.8)$$

Here $\Delta\vartheta$ is half the angular aperture of the counter.

We consider first the total cross section of the elastic process and of the inelastic processes with emission of soft quanta, the maximum energy of which, ϵ, is given by formula (3.8).

The calculation of the matrix element of order e^6 is carried out in standard fashion. In view of the technical complexity, we neglect in the calculation of the contributions of diagrams 2 and 3 (Fig. 6) the terms that do not contain the large logarithms of the type $\ln(-q^2/m^2)$ and $\ln(E/\epsilon)$. Consequently, the final expression for the total cross section of the elastic and inelastic scatterings can be written in the c.m.s. only with the indicated accuracy [14-16], namely:

$$\sigma_s(\vartheta)=\sigma_0(\vartheta)\left\{1+\frac{\alpha}{\pi}\left[4\left(1-2\ln\frac{E\sin\vartheta}{m}\right)\ln\frac{E}{\varepsilon}+\frac{22}{3}\ln\frac{E}{m}\right]\right\}. \quad (3.9)$$

Inasmuch as we are interested in large scattering angles (in practice $\vartheta \geq 30°$), we can disregard the logarithmic angle dependence in terms containing one logarithm, for example, we need not retain terms containing $\ln\sin\vartheta$ and containing no other logarithms, since these terms are of the same order as the discarded ones. Within the limits of accuracy of the formula, the angle dependence must be taken into account only in terms in which the angle logarithm is multiplied by a large logarithm.*

We should now take into account the contribution of the hard photons with energy larger than ϵ. Whereas in considering the emission of soft photons we have assumed that the photon energy is much smaller than the initial electron energy, so that the terms containing k in the numerator could be discarded in (3.6) and thus afford appreciable simplification, in the present case we must carry out an exact calculation. The exact formula for the cross section of the emission of a single photon in an electron-electron collision was obtained by means of an exceedingly complicated calculation by Garibyan [21]. This formula, naturally, leads to the result given above, namely that the photon radiation is concentrated essentially in narrow cones around the directions of motion of the initial and final electrons.

Garibyan's formula can be integrated with respect to the angles and the energies of the emitted quanta in reasonable form (under the condition that the scattered electrons strike the counters) only accurate to $\ln(E/\epsilon)$ [22,98]. In the integration with respect to the angles, the main contributions are made by the cones around the directions of the emitted electrons; the integration with respect to the energies is over the hard quanta $\epsilon < \omega < E$. As a net result we obtain

$$\sigma_h^{\mathrm{I}}(\vartheta)=\sigma_0(\vartheta)\frac{2\alpha}{\pi}\left[2\ln\frac{E}{m}\ln\frac{E}{\varepsilon}-\ln^2\frac{1}{\Delta\vartheta}-\frac{3}{2}\ln\frac{E}{m}\right]. \quad (3.10)$$

The integral cross section for the radiation of very hard quanta in the interval from E_1 to E, with $E_1 \gg \epsilon$, can be obtained with single-logarithm accuracy:

$$\sigma_h^{\mathrm{II}}(\vartheta)=\sigma_0(\vartheta)\frac{2\alpha}{\pi}\left[2\ln\frac{E}{m}\ln\frac{E}{E_1}-\ln^2\frac{1}{\Delta\vartheta}-\frac{3}{2}\ln\frac{E\Delta\vartheta}{m}+\ln^2\frac{E_1}{E\Delta\vartheta}+2\frac{E_1}{E}\left(1-\frac{1}{4}\frac{E_1}{E}\right)\ln\frac{E^2\Delta\vartheta}{mE_1}+2\int_{E_1/E}^{1-\frac{m}{E\Delta\vartheta}}\frac{dk}{k}\ln(1-k)\right]. \quad (3.11)$$

A characteristic feature of these formulas, unlike those of [16], is that in the accuracy assumed the cross section for the emission of hard quanta does not depend on the scattering angle. We note that in view of

*In considering terms that contain the angular dependence in formula (3.9), it is necessary to take account of the fact that in calculating the contributions of the inelastic scattering in formula (3.6) we discarded terms containing k in the numerator. This neglect is valid for small values of k. Actually, however, in formula (3.8) we have $\epsilon \sim$ 30-50 MeV, so that this neglect is not correct and, generally speaking, the discarded terms may produce terms with the same angular dependence as the retained terms.

the relatively large angular aperture of the counters used in the specific experiments (as was already noted in the preceding footnote), the choice of the value given by (3.8) as the soft-quantum limit is inconvenient. It is therefore necessary to choose in the correct calculation $\epsilon \sim m$, and assume all other quanta to be hard, so that formula (3.9) actually becomes correct. The total radiative corrections are obtained by adding the contributions of the soft and hard photons, and the result should be independent of the value of ϵ, the boundary between the soft and hard quanta, since this boundary is purely arbitrary. All the formulas given above are valid, of course, for arbitrarily small ϵ. For experiments with colliding beams it is particularly important to account for the dependence of the radiative corrections on the scattering angle, since what is actually measured is the differential scattering cross section in relative units, after which the resultant curve is normalized, to the theoretical curve (with account of the radiative corrections) for small scattering angles (small momentum transfers, for which quantum electrodynamics is known to be valid). It is seen from (3.9) and (3.10) that the angular dependence is contained only in the terms with $\ln(E/\epsilon)$. In [16] the value of ϵ was chosen in the form (3.8), and the dependence of the radiative corrections on the scattering angle obtained as a result of this is, for the reasons indicated above, incorrect. In view of the extremely cumbersome calculations, the correct result can be obtained by numerically integrating Garibyan's formula with the aid of an electronic computer (or else by directly calculating the corresponding diagrams on an electronic computer). The results of such calculations, for specific parameters, are listed in Table II [22,98].

We have examined in detail above the radiative corrections to the electron-electron scattering formulas. The radiative corrections calculated in analytic form, for the electron-positron scattering formulas, can be obtained by simple substitution. If the initial positron momentum is p_+ and the final one is p'_+; then we must make in the corresponding formulas the substitutions

$$\begin{aligned} p_2 &\longrightarrow -p'_+, \\ p'_2 &\longrightarrow -p_+. \end{aligned} \tag{3.12}$$

It is obvious that then

$$s^2 \longleftrightarrow q'^2, \quad q^2 \longleftrightarrow q^2. \tag{3.13}$$

If we make this substitution, then $\sin\vartheta$ in (3.9) goes over into $2\tan(\vartheta/2)$, while formulas (3.10) and (3.11) remain unchanged. Naturally, this substitution transforms $\sigma_0(\vartheta)$ into the formula for the scattering of electrons by positrons, the so called Babbha formula, the explicit form of which can be obtained from (3.1).

The procedure for calculating the radiative corrections to the cross section for the annihilation of an electron-positron pair into a photon pair is analogous to that given above. In this case, however, along with the corrections for the differential cross section, which contain, as we have seen, the characteristics of the recording instruments whenever the contributions of the real photons are taken into account, we can also calculate the corrections to the total cross section. This is connected with the integrability of the differential cross section both in this case, and in the case of Compton scattering. Although it is necessary to have for the experiment corrections to the differential cross section, the radiative corrections to the total cross section are also of interest, since the total cross section is an invariant and consequently these corrections do not depend on the reference frame or on the recording apparatus, and are objective characteristics of the process. The calculation of the total radiative corrections to the annihilation cross section is contained in [100] and is analogous to the corresponding calculations for Compton scattering [50,99]. If the total cross section is represented in the form

$$\sigma = \sigma_0(1 + \delta_T), \tag{3.14}$$

where σ_0 is the total annihilation cross section in the Born approximation, then $\delta_T = 8$ per cent when $E = 350$ MeV and $\delta_T = 14$ per cent when $E = 3.5$ BeV.

The analysis presented above shows that radiative corrections to electrodynamic cross sections at high energies are far from small and can be significant in the experiments. This circumstance is not accidental and will be considered below.

3.2. Higher radiative corrections. In the investigation of the contributions of the higher approximations of perturbation theory one must bear in mind the following peculiarity: whereas at low particle energies the perturbation-theory series is an expansion in the small parameter $e^2 = 1/137$ and converges rapidly, by virtue of which the higher terms of the series can be discarded with a high degree of accuracy, at large energies the expansion parameter is no longer e^2 but $e^2 \ln^n(E/m)$ ($n = 1$ or 2) [23-25]. In view of this, the perturbation-theory series converges slowly, at a rate that deteriorates with increasing energy, so that generally speaking a large

Table II. Radiative corrections to the electron-electron scattering cross section, $E = 500$ MeV, $\Delta\vartheta = 3.5°$

Scattering angle	40°	50°	60°	70°	80°	90°
Radiative correction	0.106	0.121	0.132	0.137	0.141	0.144

number of terms is needed in the perturbation-theory expansion. By virtue of the fact that a direct calculation of the higher approximations by the Feynman technique is extremely difficult, inasmuch as the difficulty and complexity of the calculations increases sharply with increasing order of the approximation, it is necessary to have either radically new methods, which get around perturbation theory, or an essential improvement in the convergence of the perturbation-theory series.

Calculation of electrodynamic effects without application of perturbation theory is undoubtedly very enticing. There were many attempts made in this direction. Schwinger [26,27] formulated a system of functional equations for the single-particle Green's functions; however, in view of its functional character, the system cannot be solved directly and must be reduced to a different form. One such form was developed by Ioffe, Galanin, and Pomeranchuk [28,29] and reduces to an infinite system of coupled equations. At the present time there are no satisfactory methods for solving this system. Another formulation of the system of functional equations was obtained in [30-32] and consists of the following. The space (coordinate or momentum) is replaced by a grid, and the function of the coordinates in this space is replaced by a set of values at the corners of this grid. Thus, the functional is replaced by a function of N variables (depending on the number of fields and corners). This makes it possible to obtain the basic quantities in the form of integrals with respect to these variables. In the limit the number of variables N goes to infinity, and the distances between corners tends to zero. The results of the calculations are expressed in terms of continual integrals. An approximate calculation of the continual integrals, but as applied to a problem much simpler than quantum electrodynamics (polaron theory) [33] yielded results in good agreement with those of other methods, particularly of the direct variational method. Nonetheless, the question of the possibility of approximately calculating continual integrals in the case of quantum electrodynamics remains open, particularly because of the need for eliminating the divergences.

At the same time it must be noted that there are many questions in which the expansion in e^2 is in itself perfectly admissible, but, as we have already noted, the series of the ordinary perturbation theory converges too slowly, so that an appreciable improvement in the convergence of this series is essential. Among such problems are: the asymptotic behavior of the basic functions of the theory at high energies, the infrared catastrophe, and also the effects of interest to us at higher energy.

Blank [34,35] integrated approximately the Schwinger equations with the aid of the proper-time method, and although he used expansion in e^2 during the course of the solution, this method makes it possible to improve appreciably the convergence of the perturbation-theory series.

A considerable improvement in the convergence of the perturbation-theory series can be obtained also with the aid of the renormalization-group method [36-41]. We note that individual terms in the perturbation theory expansions for the Green's functions of the electron and photon and for the vertex parts are not invariant with respect to the renormalization group, whereas the quantities themselves are invariant. A renormalization group is defined as the group of transformations

$$G_1 \to G_2 = zC_1, \quad \Gamma_1 \to \Gamma_2 = z^{-1}\Gamma_1, \quad D_1 \to D_2 = z_3 D_1, \quad e_1^2 \to e_2^2 = z_3^{-1} e_1^2, \tag{3.15}$$

the meaning of which is that the use of the quantities G_1, Γ_1, D_1, and e_1 leads to the same results as the use of the quantities G_2, Γ_2, D_2, and e_2, that is, to a description of the interaction of the electrons and photons with the same coupling constant, which can be chosen equal to its experimental value. The gist of the method is to superimpose the condition of renormalization invariance on each of the terms of the perturbation-theory series. It turns out that each term of the series obtained as a result is the sum of an infinite number of diagrams. The general solution of the Lie differential equations of the renormalization group is determined with accuracy to arbitrary functions of two arguments. Consequently, to obtain the specific form of the functions it is stipulated that the results agree with perturbation theory in case of small e^2; thus, when using the method of the renormalization group it is necessary to have calculated corrections in the lower perturbation-theory approximation.

Landau, Abrikosov, and Khalatnikov [42-45] proposed a closed system of quantum-electrodynamics equations, and took into consideration only terms containing the maximum power of the logarithm, which leads to a consideration of a definite aggregate of diagrams. Following the same path of separating the essential diagrams containing the maximum power of the logarithm, Sudakov [24,25] and Abrikosov [20,23] proposed their own method of perturbation-theory summation with logarithmic accuracy. Within the frame of this method, one retains only those diagram contributions which contain the logarithm to the highest power. It turns out that in the case of the consideration of real effects (when the vectors are time-like) these terms in n-th order of perturbation theory are the doubly-logarithmic terms of the type $[e^2 \ln^2(E/m)]^n$ (E is a quantity on the order of the energy of the particles participating in the reaction). In this method we neglect the single-logarithm terms of the type $[e^2 \ln(E/m)]^n$. It is clear that the accuracy of the method increases with the particle energy.

In scattering of electrons in colliding beams, one investigates only large-angle electron scattering.

The double-logarithmic corrections for this case were calculated in [48,49].

A general n-th order diagram, as shown in Fig. 9, was considered. We note that the parts of the diagram containing the vacuum polarization do not produce doubly-logarithmic terms and were left out, so that the diagram of Fig. 9 is the most general type of diagram that contributes in the doubly-logarithmic approximation. This diagram was considered as the skeleton diagram, into which the "overgrown" electron and photon Green's functions and the vertex parts were inserted. After several transformations,

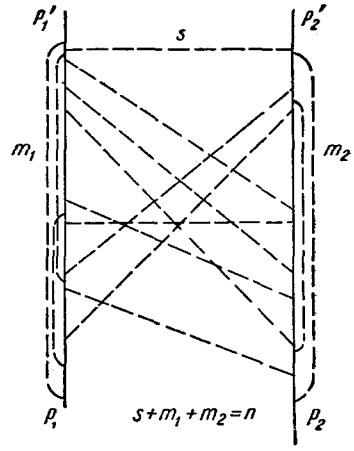

FIG. 9

the expressions for the contribution of the diagram could be reduced to a sufficiently simple form, in which it was possible to sum all the topologically-irreducible diagrams in the given n-th order. A remarkable fact was that the contributions of all diagrams containing more than one "ladder" (that is, connecting different electron lines) photon line cancel one another out. After summing with respect to n we obtain the total cross section of the elastic process in the doubly-logarithmic approximation

$$\sigma(\vartheta) = \sigma_0(\vartheta)\, e^{-4f}, \qquad (3.16)$$

where $\sigma_0(\vartheta)$ is the Moller cross section; f an integral diverging when $p_i^2 - m^2 \to 0$ (p_i is the electron momentum, and $p_i^2 - m^2$ is a measure of the energy lost by the electron to radiation). It is seen that unlike the ordinary method of eliminating the infrared divergence, where $\sigma \to \infty$ as $p_i^2 - m^2 \to 0$, in this case $\sigma \to 0$ as $p_i^2 - m^2 \to 0$. This is the result of using an improved perturbation theory and is understandable from the physical point of view, since it denotes that the cross section of a purely elastic process is equal to zero. The latter follows from the fact that the probability of emission of soft quanta in the collision tends to infinity as $\omega \to 0$.

As is well known, to eliminate the infrared divergence it is necessary to take into account the radiation of the real quanta. The total cross section of the elastic and inelastic processes can be represented in the form

$$\sigma(\vartheta) = \sigma_0(\vartheta) \exp\left\{-\frac{8e^2}{\pi} \ln\frac{E}{\Delta E} \ln\frac{E}{m}\right\}, \qquad (3.17)$$

where ΔE is the total energy carried away by the photons. We see that if $\Delta E = E$ (that is, the detector registers all the electrons regardless of their energy loss), then in the accuracy assumed the total cross section coincides with the cross section calculated in the lowest perturbation-theory approximation ($\sigma = \sigma_0$). As is well known [23] this is connected with the fact that in the doubly-logarithmic approximation the reduction in the cross section of the main process without the radiation of additional quanta, brought about by an account of the radiative corrections, is completely compensated by the increase in the contributions of the cross sections of the processes with additional multiple radiation of hard photons in the case of arbitrary radiation ($\Delta E = E$).

The importance of taking into account the doubly-logarithmic terms is connected with the fact that in the investigated energy interval, at sufficiently small ΔE (which, as we have seen in the preceding section, denotes either a detector with high energy resolution, or a counter with small angular dimensions) the doubly-logarithmic terms, meaning therefore the exponent in (3.17), turn out to be of the order of unity. At the same time, as we have already noted (3.5), the single-logarithm terms are much smaller than unity at the energies attainable at the present time, and perturbation theory accounts for them adequately.

Thus, one can conceive of two different situations: 1) the detectors have quite good energy resolution (ΔE is small). Then the most important role among the radiative corrections is played by the doubly-logarithmic corrections, processes with emission of hard photons are not registered, and the one-logarithmic terms can be taken directly from (3.9). 2) The detectors have poor energy resolution (ΔE large), and in this case the contribution of the doubly-logarithmic terms is small, so that the radiative corrections can be calculated in the e^6 order of perturbation theory. In this case a correct account is necessary of the radiation of the hard photons.

If we are interested in the emission of n real photons in the case of arbitrary radiation, then

$$\sigma_n(\vartheta) = \sigma_0(\vartheta)\, e^{-\bar{n}} \frac{(\bar{n})^n}{n!}, \quad \bar{n} = 4f; \qquad (3.18)$$

This is the Poisson distribution, showing that the radiation has a classical character, and the emission probability does not depend on the number of previously emitted quanta.

Formula (3.17) is valid also for the electron-positron scattering cross section. As regards the two-quantum annihilation of an electron-positron pair, it

is interesting to ascertain here the number of additional photons emitted along with the two main quanta. For quanta with energy larger than ΔE, this number is [49]

$$\overline{N} = \frac{4e^2}{\pi} \ln \frac{E}{m} \ln \frac{E}{\Delta E}. \quad (3.19)$$

In the case when E = 700 MeV and ΔE = 10 MeV, the average number of emitted additional quanta is $\overline{N}$ = 0.3.

The higher radiative corrections can be calculated also with the aid of the renormalization-group method [51], where it turns out that the exponent in formula (3.17) is equal to the entire lower-order correction [see (3.9)]. The renormalization-group method provides a negative answer to the question [52] of whether the exponent can contain logarithms to an intermediate power β, where β lies between 1 and 2. [53]

An advantage of the procedure indicated above for the investigation of the higher radiative corrections is the possibility of trivial generalization to include the case of electromagnetic interaction between different particles.

3.3. Radiative corrections due to strong interactions. Along with the electromagnetic corrections to the Moller formula, it is necessary to include also corrections due to the strong and weak interactions. The latter will be considered in Chapter V below. We consider here the possible contribution of strong interactions.

Inasmuch as the electrons can interact with other fields only via the photons, it is first necessary to calculate the contribution of the strong interactions to the photon Green's function, since the contribution of the meson "cloud" of the electron is quite small, owing to the dependence on very high powers of e^2.

We know [10,11] that the polarization of vacuum by the particles is invesely proportional to the squares of their masses in the case when $k^2 \ll m^2$ (k is the momentum of the photon line, in the c.m.s. $k^2 = 4E^2$; m is the mass of the particle polarizing the vacuum). In the case when $k^2 \gg m^2$ the vacuum polarization is proportional to $\ln(k^2/m^2)$. Actually the region of interest to us is intermediate, and the exact formulas must be used. For pions with $k^2 = 4m^2$ (at the threshold of a pion pair production) the contribution of the diagram with the polarization of vacuum by the pions amounts to 0.1 per cent of the contribution of the lowest-order scattering diagram, and this value increases very slowly with increasing energy. It is meaningless to take this correction into account, since the electrodynamic radiative corrections have been calculated with much lower accuracy. The situation is similar also in the case of other strongly-interacting particles, so that it remains only to investigate the contribution of the possible interactions between the particles polarizing the vacuum. We consider the consequences of resonant $\pi\pi$ interactions [16,54].

According to Kallen, the photon Green's function can be represented by

$$D^{F'}_{\mu\nu} = \frac{g_{\mu\nu}}{p^2 - i\varepsilon} + \frac{g_{\mu\nu} - \frac{p_\mu p_\nu}{p^2}}{p^2 - i\varepsilon} [\overline{\Pi}(0) - \overline{\Pi}(p^2) - i\pi\Pi(p^2)]. \quad (3.20)$$

Here $\Pi(p^2)$ is the sum over all physical states with momentum $p_m = p$:

$$\Pi(p^2) = -\frac{V}{3p^2} \sum_{p_m = p} \langle 0 | j_\mu(0) | m \rangle \langle m | j_\mu(0) | 0 \rangle; \quad (3.21)$$

$j_\mu(0)$ is the current operator and V the normalization volume. The quantity $\overline{\Pi}(0) - \overline{\Pi}(p^2)$ is defined as

$$\overline{\Pi}(0) - \overline{\Pi}(p^2) = Pp^2 \int_0^\infty \frac{\Pi(-a)}{a(p^2+a)} da. \quad (3.22)$$

If we leave in the sum (3.21) only the two-pion states for which the transition current can be represented in the form [56]

$$\langle 0 | j_\mu(0) | k_1 j,\ k_2 i \rangle = \frac{ieV^{-1}}{(4\omega_1\omega_2)^{1/2}} (k_{1\mu} - k_{2\mu}) (\delta_{j1}\delta_{i2} - \delta_{j2}\delta_{i1}) F_\pi(p^2), \quad (3.23)$$

[where i and j are the isotopic indices of the pions and $F_\pi(p^2)$ is the pion form factor], then it only remains to calculate the integral (3.22). Substituting the resonant form of the form factor (ρ meson) in the integral, we find that after taking the strong interaction into account the correction due to the pions is on the order of 1 per cent, which as before is less than the accuracy with which the radiative corrections are calculated.

3.4. Phenomenological investigation of quantum electrodynamics at small distances. Violation of quantum electrodynamics at small distances may be due to the following: 1) non-local nature of the interaction, in which case the local interaction operator $H_{loc} = eA_\mu(x) j^\mu(x)$, in which the field and the current interact at a single point, goes over into a non-local operator of the type

$$H_{nonloc} = e \int A_\mu(x) j^\mu(y) F(x - y) d^4y, \quad (3.24)$$

where the current at the point y interacts with a field in some small vicinity, defined by the function $F(x - y)$; 2) a change in the space-time geometry at small distances; 3) fields that appear only at very small distances.

We introduce a fundamental length L, defined such that at distances larger than L the factors mentioned above play no role, but starting with r = L they come into play. We estimate below the upper limit of L, and, since we can make only crude estimates, the obtained value of L will be attributed to any of the foregoing factors.

It is clear that the distances measured in the experiment are of order 1/q [see (3.2)]. More accurate estimates can be obtained either by introducing form

factors in the electron-photon vertices, or by modifying the propagation function of the electron or photon. Estimates obtained by these methods differ only by a numerical factor.

Let us consider, for the sake of being definite, the scattering of an electron by an electron (positron). In Sec. 3.2 we saw that it is necessary to consider, with a great degree of accuracy, the class of diagrams in which one photon is exchanged. Then the matrix element (Fig. 10.a) can be written in the form

$$\Gamma_\mu(p_1', p_1)\, D^{\mu\nu}(q^2)\, \Gamma_\nu(p_2', p_2). \tag{3.25}$$

The form of the vertex function Γ_μ can be determined by making the following rather general assumptions: 1) Γ_μ is a four-vector; 2) the current conservation law $(p_1' - p_1)_\mu \Gamma^\mu = 0$ holds; 3) the electron has spin 1/2,

$$\Gamma_\nu = e\left[\gamma_\nu f_1(q^2) + \frac{\mu\sigma_{\nu\lambda}}{2m} q^\lambda f_2(q^2)\right]. \tag{3.26}$$

The scalar functions $f_1(q^2)$ and $f_2(q^2)$ describe the internal structure of the electron and are relativistic generalizations of form factors of the type

$$F(p^2) = \int \varrho(r)\, e^{iqr}\, d^3r,$$

where $\rho(r)$ is the radial charge density; it is assumed that the radiative corrections are taken into account. For a particle with a point-like charge e and a point-like anomalous magnetic moment μ we have $f_1 = f_2 = 1$. If the particles are not point like,

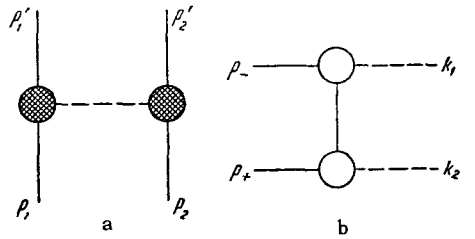

FIG. 10

then for small q^2 the functions f_1 and f_2 can be expanded in series:

$$f_{1,2} = 1 - \frac{a_{1,2}^2 q^2}{6}, \tag{3.27}$$

$$\frac{a_{1,2} q^2}{6} \ll 1. \tag{3.28}$$

If furthermore

$$\frac{q^2}{m^2} \ll 1, \tag{3.29}$$

then $a_{1,2}$ is the mean square radius of the charge distribution (of the anomalous magnetic moment distribution). Inasmuch as, unlike in the case of electron-proton scattering [59,60], the criterion (3.29) is known not to be satisfied in the region of interest to us, the indicated simple interpretation of the functions f_1 and f_2 is incorrect and both functions describe the distribution of the current-charge in the electron.

At the present time we know nothing concerning the functions f_1 and f_2, so that we assume for estimating purposes $f_2 = 0$. Then the electron-electron scattering cross section assumes the form

$$\sigma_f = \frac{r_0^2}{8\gamma^2}\left[\frac{s^4 + q'^4}{q^4} f_1^4(q^2) + \frac{2s^4}{q^2 q'^2} f_1^2(q^2) f_1^2(q'^2) + \frac{s^4 + q^4}{q'^4} f_1^4(q'^2)\right], \tag{3.30}$$

The electron-positron scattering cross section can be obtained from this by making the substitution (3.13). The exact formula with account of f_2 was obtained in [61].

Let us consider scattering through an angle $\vartheta = 90°$, $q^2 = q'^2 = -2E^2$, then

$$\sigma_f = \sigma_0\left(1 - \frac{4a^2q^2}{6}\right) = \sigma_0 - \Delta\sigma. \tag{3.31}$$

The relative deviation from the Moller cross section is

$$\frac{\Delta\sigma}{\sigma} = \frac{4a^2q^2}{6}. \tag{3.32}$$

On the other hand, it can be assumed that the vertex functions do not change, but the photon propagation function changes, [62]

$$\frac{1}{q^2} \to \frac{1}{q^2} - \frac{1}{q^2 + 1/\lambda^2},$$

which corresponds to a change in the Coulomb law

$$\frac{1}{r} \to \frac{1}{r}(1 - e^{-r/\lambda});$$

If $q^2\lambda^2 \ll 1$, then

$$\frac{1}{q^2} \to \frac{1}{q^2}(1 - q^2\lambda^2),$$

and the latter expansion is obviously not connected with the specific form of the modification of the photon propagation function. If we again consider scattering through an angle of 90°, then

$$\frac{\Delta\sigma}{\sigma} = 2q^2\lambda^2. \tag{3.33}$$

On the basis of scattering experiments only, it is generally impossible to distinguish a change in the vertex part from a change in the photon propagation function, so that both interpretations are of equal validity, and the distances at which quantum electrodynamics breaks down is a (or λ). To take both contributions into account simultaneously, we introduce the effective length

$$l^2 = \frac{a^2}{3} + \lambda^2. \tag{3.34}$$

In order to observe a deviation $\Delta\sigma$, it is necessary to measure with accuracy not lower than $\delta\sigma = \Delta\sigma/2$, then the length l, measured in experiments on electron-electron scattering through 90°, is

$$l = \frac{E_0}{E}\sqrt{\frac{\delta\sigma}{2\sigma_0}} \cdot 10^{-13}\ \text{cm}, \tag{3.35}$$

where $E_0 = 197$ MeV. The measured distances for

Table III. Effective distances l, measured at a given experimental accuracy and at a given electron energy, in units of 10^{-13} cm.

$\frac{\delta\sigma}{\sigma}$	E, MeV			
	100	300	500	1500
0.10	0,44	0.15	0.09	0,03
0.05	0.32	0.10	0.06	0.02
0.03	0.24	0.08	0.05	0.02
0.01	0.14	0.05	0.03	0.01

certain energies and accuracies are listed in Table III.

To detect deviations from quantum electrodynamics at small distances, there is no need for carrying out the very complicated measurements of the absolute cross sections. Inasmuch as $q \sim 0$ in small-angle scattering, it is sufficient to carry out the measurements of the relative cross sections, normalizing them at small angles to the Moller curve, with account of the radiative corrections.

The use of electron-positron scattering to check the validity of quantum electrodynamics at small distances offers some new possibilities: 1) the investigation of the form factors in the time-like domain [$f(s^2)$, $s^2 > 0$]; 2) measure shorter lengths, other conditions being equal, this being connected with the possibility of investigating scattering through angles larger than 90°; to be sure, the cross section of scattering through these angles is appreciably smaller than the corresponding Moller cross section[49].

Investigation of the process $e^+ + e^- \to 2\gamma$ (Fig. 10b) enables us to determine the electron propagation function $G(p)$ and the vertex part, which, generally speaking, should be written in the form $\Gamma_\mu(p^2, p'^2, k^2)$. Compared with the case of electron-electron scattering, where we investigate the function $\Gamma_\mu(m^2, m^2, k^2)$, in the case of annihilation we are investigating the function $\Gamma_\mu(p^2, m^2, 0)$, that is, the vertex part in another domain of the arguments. This is precisely why a study of the annihilation process is of very great interest for a check on the applicability of quantum electrodynamics at small distances. It must be noted that in this case the phenomenological analysis is more complicated than that given above, since, first, two scalar functions appear in $G(p)$, and, second, there is no analog of (3.26).

The form factors in the time-like domain of the arguments can be investigated also in polarization experiments that are sensitive to small-distance interactions.

Let us proceed now to an estimate of the upper limit of the length L, up to which quantum electrodynamics is known to be applicable. We shall list below the experiments on whose basis this estimate can be made.

Hofstadter's experiments[59,60] on the electromagnetic structure of nucleons have made it possible to determine the structural functions $F_1(q^2)$ and $F_2(q^2)$ over a wide range of values of momentum transfer q. If we assume that the deviations of the functions F_1 and F_2 from unity are due not only to the nucleon meson cloud but also to violation of quantum electrodynamics, then

$$\langle r^2\rangle_{obs} = \langle r^2\rangle_p + 6l^2 = (0{,}8\cdot 10^{-13}\,\text{cm})^2, \quad l \leqslant 0{,}3\cdot 10^{-13}\,\text{cm}. \tag{3.36}$$

It is obvious that an appreciable portion of the effect is due to the nucleon meson cloud, so that we can assume that Hofstadter's experiments imply the validity of quantum electrodynamics up to distances on the order of $(1-2)\times 10^{-14}$ cm.

In calculating the anomalous magnetic moment of the electron (muon), integrals are obtained with respect to the momenta of the virtual photons. If we assume that quantum electrodynamics breaks down at a distance l, then the radiative corrections to the magnetic moment assume the form[63]

$$\frac{a}{2\pi}\left(1-\frac{2}{3}l^2m^2\right). \tag{3.37}$$

In view of the large mass, the use of the muons is preferable. The latest measurements of the anomalous magnetic moment of the muon have shown that experiment agrees with theory accurate to 0.5 percent of the radiative correction, that is, $(2/3)\,l^2m^2 \leq 0.5 \times 10^{-2}$, hence $l \leq 1.5\times 10^{-14}$ cm.

These distances are indeed the minimum distances to which the applicability of quantum electrodynamics was measured; consequently, $L \leq 1.5\times 10^{-14}$ cm.

The value of the Lamb shift is also sensitive to cutoff at large momentum. In accordance with the latest data[65,101], theory agrees with experiment within 0.1 Mc, hence $l \leq 3\times 10^{-14}$, and the aggregate of data on hydrogen hyperfine structure[66] leads to $l \leq 5\times 10^{-14}$ cm.

Experiments on the verification of quantum electrodynamics with the aid of the reaction $\gamma + p \to e^+ + e^- + p$ in the case of pair production at large angles[67,68] are being carried out at the present time[69]. However, the two diagrams (on which the photon is absorbed and emitted by a proton) cannot be reduced to the Hofstadter form factors, and their estimates (strong interactions!) can be made only theoretically.

In conclusion it must be noted that in the region that will be measured in the nearest future (energies up to 700 MeV, accuracy not higher than 2—3 per cent), there are no characteristic parameters that would point to the possibility of breakdown of quantum electrodynamics at these distances. However, the observation of a breakdown of quantum electrodynamics would be of all the more interest here. As regards the suggestions advanced frequently in recent times (see, for example[70]) that the fundamental length is connected with weak interactions, the corre-

sponding distances (6×10^{-16} cm) can be eventually measured, apparently, in experiments with colliding beams. For this purpose it is necessary, for example, to carry out an experiment in colliding electron-positron beams with two BeV energy and 1 per cent accuracy.

IV. CREATION OF PARTICLES IN ELECTRON-POSITRON COLLISIONS AND INVESTIGATION OF THEIR STRUCTURE

Experiments on the creation of elementary particles upon annihilation of an electron-positron pair seem to us to be unique both with respect to the amount of information on interactions between elementary particles, and with respect to its importance. The cross sections of the corresponding processes are of the same order in the electromagnetic interaction constant e^2 as is the cross section for elastic scattering. Therefore all these processes are perfectly observable.* We shall list below the possible experiments on particle production in the annihilation of an electron-positron pair, indicating the information that can be extracted from them. We shall then consider some of these experiments in greater detail.†

1. A check whether there exist charged particle pairs (other than those hitherto discovered) independently of the properties of these particles with respect to strong interactions, if their mass is smaller than the limiting beam energy and their lifetime is not less than 10^{-9}—10^{-10} sec. These particles can be observed directly. In the case of a shorter lifetime, their decay products will be observed.

2. A check on the existence of strongly-interacting particles, including neutral particles, based on the anomaly in the cross sections of other processes and threshold effects.

3. The $e^+ + e^- \to \pi^0 + \gamma$ process, and the investigation of unstable neutral particles, the lifetime, and the electromagnetic form factor of the π^0 meson. The reaction threshold is 70 MeV.

4. The process $e^+ + e^- \to \mu^+ + \mu^-$, investigation of the muon form factor, the threshold effect, bimuonium, radiative corrections. Reaction threshold 106 MeV.

5. The process $e^+ + e^- \to \pi^+ + \pi^-$, investigation of electromagnetic form factor of the pion for time-like momentum transfers, the associated $\pi\pi$ interaction and unstable neutral particles, the investigation of radiative corrections. Threshold 140 MeV.

6. The process $e^+ + e^- \to \pi^+ + \pi^- + \pi^0$, investigation of the pion form factor, study of $\pi\pi$ interactions in other (compared with process 5) isotopic and spin states, investigation of ω and η mesons. Threshold 210 MeV.

7. The process $e^+ + e^- \to K^+ + K^-$ ($K^0 + \tilde{K}^0$), investigation of electromagnetic form factor of the K meson, and of KK and πK interactions. Threshold 494 MeV.

8. Process $e^+ + e^- \to 2K + \pi$, investigation of πK interaction, and of the K′ meson. Threshold 564 MeV.

9. The process $e^+ + e^- \to p + \tilde{p}(n + \tilde{n})$, investigation of electromagnetic form factors of nucleons for time-like arguments (unlike the Hofstadter's experiments, where the space-like momentum transfer region was investigated). Threshold 940 MeV.

10. The process $e^+ + e^- \to X + \tilde{X}$ (hyperon-pair production), investigation of electromagnetic form factors of hyperons and πX interaction.

11. Processes with production of $X\tilde{X}\pi$ for the investigation of πX interactions of different hyperon resonances (Y_0^*, Y_1^*, Y_0^{**}).

12. Processes with production of K mesons and hyperons (for example $\Sigma^-\tilde{n}K^+$), for the investigation of the corresponding interactions and resonances.

The listed experiments are among the most direct experiments with which it is possible to determine directly the properties of the elementary $\pi\pi$, πK, KK, and πX interactions. Recently these interactions have been widely investigated in many other experiments, particularly in processes with annihilation of a proton-antiproton pair. The latter are analogous to some degree with the experiments on electron-positron annihilation. In all other experiments it is necessary to separate the strong interaction of the reaction products in the final state, something that can be done only crudely and far from unambiguously. Although the particle-production cross section in the annihilation of a nucleon-antinucleon pair is four orders of magnitude larger than the particle production cross section in electron-positron annihilation, the accumulation of statistics in the latter experiments can be much faster, since the difference in the intensities of the anitproton and positron beams is much larger. The advantage of experiments with electron-positron colliding beams lies also in the fact that the measurements can be carried out over the entire energy spectrum, whereas in experiments with nucleon-antinucleon annihilation there is a threshold near 2 BeV, so that a considerable region of great interest becomes unphysical.

Let us make, finally, a remark concerning the quantum numbers of the final states. We consider processes in the lowest electrodynamic approximation, that is, when the electron-positron pair goes over into a photon which then decays into the final reaction products (Fig. 11). In the c.m.s. the virtual photon is at rest, as it were, k = (2E,0); since, on

*The particle-pair production cross section in electron-electron collisions contains the additional factor e^4 and in the case of production at large angles is 10^4 times smaller. These cross sections can be large only in the case of production at small angles, but the colliding-beam technique does not permit observation at small angles.

†This group of problems is considered also in [108].

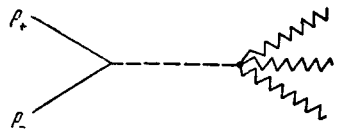

FIG. 11

the other hand, $k_\mu a^\mu = 0$, it is clear that $a_4 = 0$; consequently, the virtual photon is described by a polar vector. It follows therefore that the angular momentum of the intermediate state is J = 1 (vector particle), the parity is P = −1, and the parity with respect to charge conjugation is C = −1. Inasmuch as all these characteristics are conserved in electromagnetic and strong interactions, all the final states which are obtained upon annihilation of an electron-positron pair (accurate to radiative corrections) have the aforementioned quantum numbers.

4.1. Muon pair production. In the preceding chapter we have seen that, with a high degree of accuracy, muons are subject only to electromagnetic interactions [64]. The cross section for the production of a muon pair in the annihilation of an electron-positron pair has in second order perturbation theory (Fig. 12) the form

$$\sigma_0(\vartheta) = \frac{r_0^2}{16\gamma^2}\frac{q}{E}\left[1 + \frac{\mu^2}{E^2} + \frac{q^2}{E^2}\cos^2\vartheta\right]. \qquad (4.1)$$

Here q is the muon momentum and ϑ is the angle of muon emission relative to the direction of the electron motion.

The doubly-logarithmic corrections to the production cross section are calculated in the same manner as the corrections considered in the preceding chapter for the electron-electron scattering cross section [71]. In exactly the same way, only diagrams with a single ladder line make a contribution. An account of the radiation of the real quanta leads to a dependence of the cross section on the maximum energy ΔE carried away by the quanta; however, in view of the jump in mass $\Delta E \leq E - \mu$ and in the case of arbitrary radiation (when the detector registers all the muons, regardless of their energy) we have $\Delta E = E - \mu$. This case therefore differs in principle from the scattering and annihilation into photons, which was considered in the preceding chapter, where in the case of arbitrary radiation the reduction in the cross section of the main process (without emission of additional quanta) due to an account of the radiative corrections is completely offset by the increase in the cross sections of the processes with multiple additional photon radiation. In the present case, however,

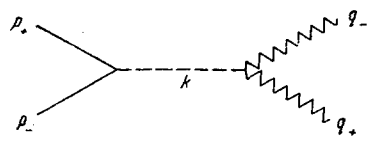

FIG. 12

no such compensation takes place, and in the case of arbitrary radiation we have

$$\sigma(\vartheta) = \sigma_0(\vartheta)\varphi^2(4E^2)\exp\left\{-\frac{4e^2}{\pi}\ln\frac{E}{E-\mu}\ln\frac{E}{m}\right\}, \qquad (4.2)$$

where $\varphi(4E^2)$ is the muon form factor which, as we have already noted, is equal to unity in the space-like domain, and μ is the muon mass. It is clear that the effect is most noticeable at the threshold, when $E \gg E - \mu$. For nonrelativistic muons (near threshold) formula (4.2) can be rewritten in the form

$$\sigma(\vartheta) = \sigma_0(\vartheta)\varphi^2(4E^2)\left(\frac{q}{\sqrt{2\mu E}}\right)^{\frac{8e^2}{\pi}\ln\frac{E}{m}}|\psi(0)|^2, \qquad (4.3)$$

and the factor $|\psi(0)|^2$ takes into account the Coulomb interaction of the final muons, which likewise is significant near threshold [72]:

$$|\psi(0)|^2 = \frac{\frac{2\pi e^2}{v}}{1 - e^{-\frac{2\pi e^2}{v}}}. \qquad (4.4)$$

Both the foregoing effects change the dependence of the cross section of the process on the momentum of the outgoing particles. In the region where the Coulomb interaction is insignificant ($2\pi l^2/v \ll 1$) we obtain $\sigma \sim q^{1.1}$ in place of $\sigma \sim q$.

The Coulomb interaction between the produced muons can lead to the formation of a bound state of positive and negative muons—bimuonium [73]. Bimuonium can decay not only into photons (the lifetime of parabimuonium is $\sim 0.6 \times 10^{-12}$ sec) but also into an electron-positron pair (lifetime of orthobimuonium is $\sim 2 \times 10^{-12}$ sec). The scattering of an electron by a positron and the annihilation of an electron-positron pair into photons can proceed via the aforementioned intermediate bound state. Therefore investigation of bimuonium is of interest not only for a study of the properties of muons, but also as an example of an unstable intermediate state which is amenable to exact calculation. In this case a very narrow ($\sim 10^{-3}$ eV) and a very high ($\sim 10^{-25}$ cm^2) peak appears in the cross section. We note that the cross section without account of this effect is $\sim 10^{-31}$ cm^2. Because of the scatter in the particle energy in the colliding beams, this effect becomes smeared out, nonetheless it can be observed under certain conditions [73].

4.2. Creation of pions in electron-positron collisions. Of exceptional interest is the investigation of $\pi\pi$ interaction as one of the fundamental interactions. This interaction contributes to the cross section of many processes in which pions and baryons participate. Data on this interaction are obtained at the present time from an analysis of the reactions $p + \tilde{p} \to n\pi$, $\pi + p \to 2\pi + p$, and many other processes. It follows from these experiments that the $\pi\pi$ interaction indeed exists and has a resonant character.

One of the most direct methods of investigating the $\pi\pi$ interaction is the reaction

$$e^+ + e^- \to n\pi, \qquad (4.5)$$

which yields information on the vertex $\gamma \to n\pi$ and consequently on the electromagnetic form factor of the pion, which can be connected with the phase shifts of the $\pi\pi$ scattering. In addition, the electromagnetic form factor of the pion is in itself a fundamental quantity and is contained in the cross sections of other processes.

As was already noted, accurate to radiative corrections, the final pions are in a state with J = 1, P = −1, and C = −1. In addition, a system of n pions has a definite G parity, $(-1)^n$. In electromagnetic transitions, in the lowest order, the isotopic spin either remains constant or changes by unity. Therefore, accurate to radiative corrections, the isospin of the n created pions is either 0 or 1. Taking into account that $G = CT_2$ and C = −1, we obtain $T_2 = (-1)^{n-1}$. Thus, for an even number of pions we obtain an isotopic spin 1 (an isotopic vector, which reverses sign upon the rotation T_2), while for an odd number of pions we obtain isospin 0 (an isotopic scalar, which does not reverse sign upon the rotation T_2). From the fact that in the final state C = −1 it follows, in particular, that a process in which all the final particles are neutral pions is forbidden.

We are interested in the transition current

$$\langle q^1, q^2, \ldots, q^n | j_\mu(0) | 0\rangle = \frac{1}{(2\pi)^{3n/2}} J_\mu(q^1, q^2, \ldots, q^n), \quad (4.6)$$

where q^i are the momenta of the created pions. From the current conservation law it follows that $k_\nu J^\nu = 0$; inasmuch as the spatial part of k is equal to 0 in the c.m.s., it follows that $EJ_4 = 0$. We shall therefore consider only the spatial component of the transition current **J**. Since **J** is multiplied by a polar vector, it follows from the parity-conservation law that **J** is a polar vector made up of the vectors $\mathbf{q}^1, \mathbf{q}^2, \ldots, \mathbf{q}^n$ if n is even, and an axial vector if n is odd. Taking this into account, we readily obtain the cross section [80]

$$\sigma_{n\pi} = \frac{e^2}{32E^4} \frac{1}{(2\pi)^{3n-5}} \times \int \prod_{i=1}^{n} d\mathbf{q}_i \delta\left(\sum_i \omega_i - 2E\right) \delta\left(\sum_i \mathbf{q}_i\right) |\mathbf{J}|^2 \sin^2\vartheta, \quad (4.7)$$

since in the initial state there is only one vector—the collision direction; ϑ is the angle between the collision line and the vector **J**. Thus, the angular distribution follows only from the gauge invariance and does not depend on the properties of the vertex $\gamma \to n\pi$. In the case of the creation of two pions, there is a unique vector $\mathbf{J}(\mathbf{q}^1 = -\mathbf{q}^2)$, and the angular distribution is completely determined by the factor $\sin^2\vartheta$. In the case of the creation of three pions, **J** should be proportional to the axial combinations $(\mathbf{q}^1 \times \mathbf{q}^2) = -(\mathbf{q}^1 \times \mathbf{q}^3)$ etc.; it follows therefore that the vector **J** is normal to the plane of creation and consequently the angular dependence of the cross section on the angle between the normal to plane of creation and the collision line is again $\sin^2\vartheta$.

In the case when two pions are created, they are created in a state with relative angular momentum $l = 1$. The cross section of the process is

$$\sigma_{2\pi}(\vartheta) = \frac{r_h^2}{3\gamma^2} \frac{q^3}{E^3} \sin^2\vartheta F_\pi^2(4E^2). \quad (4.8)$$

Thus, it is possible to measure directly in the experiments the isovector electromagnetic form factor of the pion, $F_\pi(s)$. The region where the form factor is determined for different processes is shown in Fig. 13. In experiments on pion-pair production the form factor is investigated in the time-like region, while the form in the space-like region can be measured in principle in experiments on the scattering of pions by electrons.

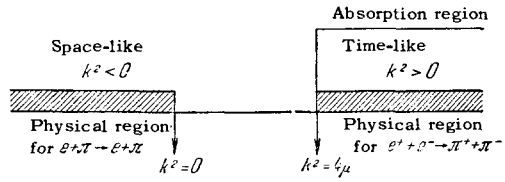

FIG. 13

In the interval $s < 16\mu^2$, the form factor $F_\pi(s)$ can be expressed in terms of the $\pi\pi$ scattering phase shift in a state with isotopic spin 1 and angular momentum 1

$$F_\pi(s) = e^{\frac{s}{\pi}\int_{4\mu^2}^{\infty} \frac{\delta_{11}(s')\,ds'}{s'(s'-s)}}. \quad (4.9)$$

The form factor $F_\pi(s)$ was first investigated theoretically, particularly within the framework of the Mandelstam representation [81-83] and in many investigations [57,58,77] a resonant form of $\pi\pi$ interaction was obtained for certain values of the parameters, leading to the appearance of sharp peaks in the function $F_\pi(s)$. Even the first analysis of the experiment has confirmed qualitatively [79,84-87] the resonant character of the $\pi\pi$ interaction. Such an interaction can be described as an unstable meson with T = J = 1 and negative parity, which rapidly decays into a $\pi^+\pi^-$ pair. The recently discovered ρ meson [102,103] and ζ meson [104] have precisely these properties, and consequently the form factor as a function of the energy will have at least two peaks. The simplest form of the function $F_\pi(q^2)$ takes into account only the indicated resonant interactions (pole diagrams) of Fig. 14a;

$$F_\pi(q^2) \sim \frac{m_\varrho^2}{q^2 - m_\varrho^2 - im_\varrho\Gamma_\varrho} + \frac{m_\zeta^2}{q^2 - m_\zeta^2 - im_\zeta\Gamma_\zeta}. \quad (4.10)$$

It must be noted that the indicated resonances have not yet been sufficiently investigated, and experiments with colliding electron-positron beams, in which high energy resolution can be obtained, could provide the

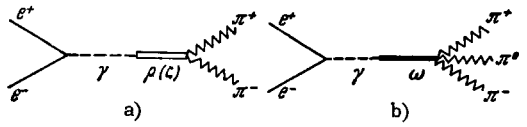

FIG. 14

exact form of the peaks, and in particular would make it possible to determine whether the ρ^0 meson splits up into two [105]. Naturally, formula (4.10) does not hold in the nonresonant region. A study of the form factor in this region is also of interest, since this method makes it possible to determine directly the phase shifts of the $\pi\pi$ scattering, something particularly valuable near threshold, since the absorptive cut begins directly at the threshold, while the region of many particles is located sufficiently far away.

To estimate the heights of the peaks it is necessary to know the level widths of the ρ and ζ meson. If we put $m_\rho = 750$ MeV, $\Gamma_\rho \sim 100$ MeV and $m_\zeta = 575$ MeV, $\Gamma_\zeta = 70$ MeV, then the height of the ρ-meson peak is ~ 60 (compared with $F_\pi = 1$), while the height of the ζ-meson peak is ~ 70. The form of the dependence of the form factor $|F_\pi(q^2)|$ on the momentum transfer is shown in Fig. 15.

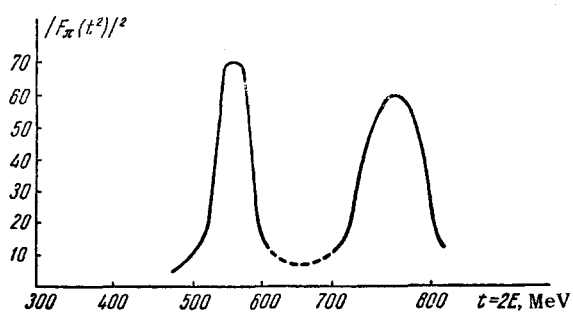

FIG. 15

The three pions (π^+, π^0, π^-) are created in states $L = l = 1$, $L = l = 3$, $L = l = 5$, etc., where l is the relative angular momentum of the positive and negative pions and L is the relative angular momentum of the π^0 meson, referred to the center of mass of the $\pi^+\pi^-$ system. The transition current (4.6) can be represented in this case in the form

$$J^\nu(q^+, q^0, q^-) = \frac{-ie}{\sqrt{8\omega_+\omega_-\omega_0}} \varepsilon^{\nu\alpha\beta\gamma} q_\alpha^+ q_\beta^- q_\gamma^0 H(E, \omega_+, \omega_-). \quad (4.11)$$

The isoscalar form factor of the pion H is a function of three variables (we choose E, ω_+, ω_-). The vector J has the form

$$\mathbf{J} = 2\frac{eE}{\sqrt{8\omega_+\omega_-\omega_0}} (\mathbf{q}^+ \times \mathbf{q}^-) H(E, \omega_+, \omega_-). \quad (4.12)$$

With our choice of independent kinematic parameters, the cross section can be represented in the form

$$\frac{d^3\sigma}{d\Omega\, d\omega_+\, d\omega_-} = \frac{e^4}{(2\pi)^3} \frac{H^2}{64E^2} |(\mathbf{q}^+ \times \mathbf{q}^-)|^2 \sin^2\vartheta, \quad (4.13)$$

where, as already noted, ϑ is the angle between the collision line and the normal to the creation plane.

The isoscalar form factor of the pion H plays an important role in explaining the isoscalar part of the electromagnetic form factors of nucleons. A theoretical investigation of this form factor is very difficult. However, appreciable information on the properties of the form factor can be gained from the fact that the ω and η mesons exist [102,106] (if the η meson is a vector particle [106]). In fact (see Fig. 14b), a virtual photon can go over into an ω (or η) meson, which then breaks up into three pions. If we take into account only such pole diagrams then, as in the case of the form factor $F_\pi(q^2)$, we can estimate the dependence of the form factor H(E) on the momentum transfer only in the resonant region (Fig. 16). The peaks of the form factor H(E) are much narrower than those of the form factor $F_\pi(q^2)$, inasmuch as the level widths of the ω and η mesons are appreciably smaller than those of the ρ and ζ mesons, and according to many estimates amount to ~ 0.3 MeV [107].

4.3 Processes in which π^0 mesons participate. The decay of a π^0 meson into two photons can be described with the aid of the phenomenological interaction

$$H_{\text{int}} = \frac{1}{\mu}\sqrt{\frac{8\pi}{\mu\tau}}\, \varphi(x)\, \varepsilon_{\alpha\beta\gamma\delta} \frac{\partial A^\alpha(x)}{\partial x_\beta} \frac{\partial A^\gamma(x)}{\partial x_\delta}. \quad (4.14)$$

Of great interest are processes in which one of the photons is virtual. In these processes it is possible to investigate the electromagnetic form factor of the π^0 meson. The three processes shown in Fig. 17 cover the entire region of momentum transfer of the function $\Gamma_{\pi 0}(k^2, 0, \mu^2)$. In experiments with colliding beams it is possible to use the process $e^+ + e^- \to \pi^0 + \gamma$ (see the diagram of Fig. 18), the cross section of which is [74-76]

$$\sigma_{\pi^0\gamma}(\vartheta) = \frac{e^2}{4\tau\mu^3} \frac{q^3}{E^3} (1 + \cos^2\vartheta)\, g^2(4E^2); \quad (4.15)$$

Here τ is the lifetime of the π^0 meson ($\tau = 2 \times 10^{-16}$

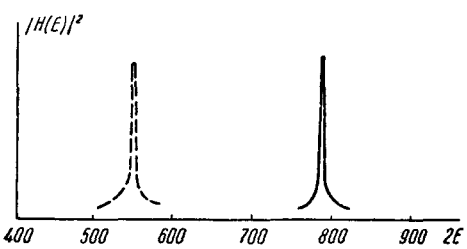

FIG. 16

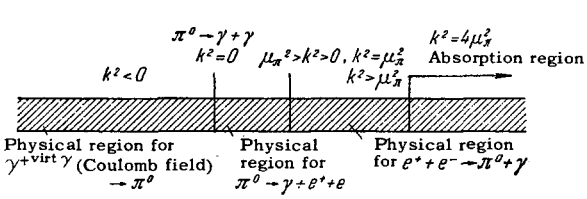

FIG. 17

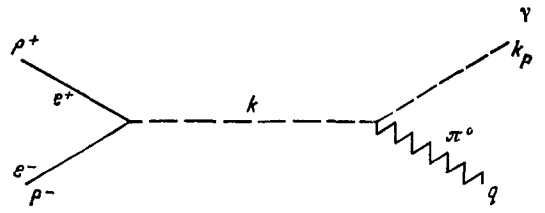

FIG. 18

sec), μ is its mass, and q is the momentum, and $g(4E^2) = \Gamma_{\pi 0}(4E^2, 0, \mu^2)$. An investigation of a process with production of π^0 and γ is quite difficult because of the difficulty in observing three photons and because of the small cross section, which does not exceed 10^{-35} cm^2 if the form factor is not taken into account; this is connected with the relatively large lifetime of the π^0 meson compared with the characteristic electromagnetic time. However, an account of the new resonances changes the situation radically: the virtual photon can go over into any one of four mesons, ω, η, ρ, and ζ, and any of these can decay into a π^0 and γ. Moreover, according to the available data [106], the probability of an η-meson decay into π^0 and γ is three times larger than the probability of a decay into three pions. Therefore the cross section of the process with production of π^0 and γ turns out to be of the same order as the cross section for the production of three pions (or two pions) and can reach 10^{-29}—10^{-30} cm^2 in the resonances. Thus, a process with formation of π^0 and γ can be used to investigate unstable neutral mesons, the quantum numbers of which coincide with the quantum numbers of the virtual photon.

4.4. Production of K mesons and baryons in electron-positron collisions. The electromagnetic form factor of the K mesons can be investigated in the reaction $e^+ + e^- \to K^+ + K^-$; the cross section of this process is given by formula (4.8), but now F denotes the electromagnetic form factor F_K of the K meson. A theoretical investigation of the form factor F_K is quite difficult, since apparently it is determined to a considerable degree by the πK interaction, about which practically nothing is known at present. Information concerning this interaction can be obtained also from the process $e^+ + e^- \to 2K + \pi$, in which K′ resonance (a K′ meson) will appear.

Along with the charged K mesons, there can be created pairs of neutral K mesons (unlike the creation of neutral pions). Inasmuch as the pair $(K_0, \tilde{K}_0)$ should be in a state with charge parity $C = -1$, the final-state function should have the form $K_0\tilde{K}_0 - \tilde{K}_0K_0$; changing over to K_1^0 and K_2^0 mesons, we obtain $K_1^0K_2^0 - K_2^0K_1^0$. It is clear therefore that only the pair $K_1^0 - K_2^0$ can be created, but not the K_1^0-K_1^0 or the K_2^0 - K_2^0 pairs.

The cross section for the production of a pair of fermions with spin 1/2 in the annihilation of an electron-positron pair has the form

$$\sigma_f(\vartheta) = \frac{r_0^2}{16\gamma^2}\frac{q}{E}\left\{|F_1(4E^2) + \mu F_2(4E^2)|^2(1+\cos^2\vartheta) + \sin^2\vartheta\left|\frac{M}{E}F_1(4E^2) + \frac{E}{M}\mu F_2(4E^2)\right|^2\right\}, \quad (4.16)$$

Here μ is the static anomalous magnetic moment and F_1 and F_2 is the analytic continuation of the electric and magnetic form factors of the fermion into the region of time-like momentum transfers. Figure 19 shows the situation for the special case of the isovector part of the electromagnetic vertex of the nucleon.

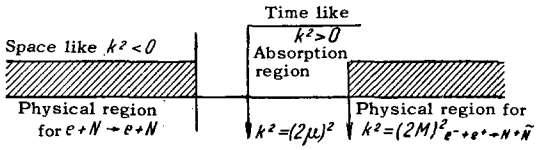

FIG. 19

The form factors have an imaginary part along the absorption cut. This gives rise to fermion polarization normal to the creation plane. We note that in the process e + f → e + f this polarization cannot be produced, accurate to radiative corrections, as follows from the invariance with respect to time reversal. The fermion polarization is given by the formula

$$P(\vartheta) = -\sin 2\vartheta\,\frac{q^2}{EM}\,\mathrm{Im}\{F_1^*(4E^2)\,\mu F_2(4E^2)\}; \quad (4.17)$$

the polarization of the antifermion is $-P(\vartheta)$, as follows directly from the CPT theorem.

The final pair of particles is produced in states $^3S_1$ and $^3D_1$, as follows from parity conservation and from the fact that the total angular momentum is equal to 1. As regards the isotopic structure of the vertex γff, it breaks up into an isoscalar and isovector part (for the Λ and Σ^0 hyperons there is only the isoscalar part). The absorption cut begins with $4\mu^2$ for the isovector part and with $9\mu^2$ for the isoscalar part. An exception is the $\gamma\Sigma\tilde{\Sigma}$ vertex, for which the transition $\Sigma \to \Lambda + \pi$ leads to an anomalous threshold [89]. An investigation of the electromagnetic form factors of the nucleons in the time-like region is of very great interest, since one cannot exclude the possibility that the nucleon core presently observed in experiment is connected with singularities at large positive k^2.

Along with creation of the fermion-antifermion pair, the reactions $e^+ + e^- \to \Sigma^0 + \tilde{\Lambda}$ or $\tilde{\Sigma}^0 + \Lambda$ are also possible. The cross section of this process depends on the relative parity of Σ-Λ. This effect can be investigated directly by observing the behavior of the production cross section at threshold. In fact, if the relative parity of Σ-Λ is positive, then the final particles are produced in states $^3S_1$ and $^3D_1$; on the other hand, if it is negative, then the final states will be $^1P_1$ and $^3P_1$. Consequently, for positive parity the cross section increases linearly with the final mo-

mentum q and is isotropic, whereas for negative parity it increases as q^3 and generally speaking contains terms of the type $\cos^2\vartheta$.

If we leave out the terms with anomalous magnetic moment, then the cross section (4.16) decreases as E^{-2}, while the terms with the anomalous magnetic moment are multiplied by a rapidly decreasing form factor [60]. As a result of this the cross sections for baryon production are small ($\sim 10^{-33}$ cm^2), and the observation of the corresponding processes is quite a complicated problem.

4.5. Detection of the existence of new particles. As we have already noted, experiments with colliding beams can be used for the detection of particle-antiparticle pairs, both charged and neutral.

We have already given the cross sections for the production of particles with spin 0 (4.8) and with spin 1/2 (4.16). The cross section for the production of a particle with spin 1 (vector boson with anomalous magnetic moment μ_B) is [108]

$$\sigma_B(\vartheta) = \frac{r_0^2}{32\gamma^4}\frac{q^3}{E^3}\left\{2(1+\mu_B)^2\left(\frac{E}{m_B}\right)^2(1+\cos^2\vartheta) + \left[2+\left(\frac{E}{m_B}\right)^4\left(\frac{m_B^2}{E^2}+2\mu_B\right)^2\right]\sin^2\vartheta\right\}. \quad (4.18)$$

The search for the intermediate vector boson of weak interaction is of great interest. We note that such a boson should have a proper quadrupole moment and, generally speaking, is characterized by three form factors [108].

Even if we exclude terms with anomalous magnetic moment and with quadrupole moment, which increase as E^2, the cross section for the production of the vector boson does not decrease with energy. This is connected with the non-normalizable character of the interaction. Inasmuch as, accurate to the radiative corrections, the angular momentum of the final state is equal to 1, only the lower waves contribute in this approximation and from unitarity considerations the cross section cannot exceed $3\pi\lambda\!\!\!^{-2}/4$. Therefore, starting with certain energies, the cross section should decrease, something that can be ensured by the form factors. If formula (4.18) has a certain region of applicability (a region where the form factors are of no significance), then the cross section for the production of the vector boson may become larger than the other cross sections. Because of the short lifetime ($\sim 10^{-17}$ sec), a vector meson can be observed only by its decay products.

Experiments with colliding beams are very convenient for the separation of neutral (bound) resonant states (or unstable mesons). We have already seen this with the form factor resonances and bimuonium as an example. Let us consider this question in general. Assume that annihilation of an electron-positron pair is accompanied by the production of a resonant state with mass M, spin J, and decaying with a relative probability Γ_i at a total level width Γ. We have to consider different ratios between the level width Γ and the energy resolution ΔE: 1) narrow resonance, $\Delta E > \Gamma$; 2) broad resonance, $\Delta E < \Gamma$; 3) intermediate case, $\Delta E \sim \Gamma$. The resonant contribution to the process $e^+ + e^- \to$ final state, averaged over the interval ΔE, will be: for case 1) $\sigma_{av}^{I} = 2\pi\lambda\!\!\!^{-2}(\pi/4) \times (2J+1)\Gamma_f\Gamma_i(\Gamma/2\Delta E)$; for case 2) $\sigma_{av}^{II} = \pi\lambda^2(2J+1)\Gamma_f\Gamma_i$; for case 3) we can use either of the formulas. It is simplest to observe the resonant state with $J = 1$ and $C = -1$, as we have seen above. The contributions of resonances with other quantum numbers will contain an excessive smallness in e^2 (for in this case at least two photon lines must participate), thus $\Gamma_i \sim e^8$ for $J = 1$, $C = 1$, etc.

V. INVESTIGATION OF WEAK INTERACTIONS IN EXPERIMENTS WITH COLLIDING BEAMS

A characteristic feature of the theory of local weak interactions is the quadratic increase of the cross sections with the energy. Therefore cross sections that are very small at low energies, may become comparable with the cross sections for the electromagnetic and strong interactions at high energies. However, from the general premises of modern theory [91,109] it follows that the cross section of any process at large energies should not grow more rapidly than $\ln^2 E$. It is very important to establish where the growth of the cross sections of the weak interactions with energy is reduced. At those energies the form factors enter into play, and a study of these form factors is of great interest, particularly since this may be a manifestation of the fundamental length.

Colliding-beam techniques may produce energies so high that, at least in principle, weak interactions at high energies can be investigated.

As is well known, all the available experimental data are well described by the V-A weak-interaction scheme [92]. In this scheme we retain only charged currents, which describe the scattering of charged particles by neutral ones. It is possible, however, to include in this scheme also neutral currents, which describe the scattering of particles of like charge. The scheme obtained is quite symmetrical and simple, and is also in good agreement with all the available experimental data [93,94]. Let us consider within the framework of the scheme with neutral currents the processes that can be investigated with colliding beams [94].

We consider the influence of weak interactions on the scattering $e + e \to e + e$ and annihilation $e^+ + e^- \to \mu^+ + \mu^-$ and $e^+ + e^- \to N + \bar{N}$ processes.

The total cross section of each of these processes can be represented in the form

$$\sigma = \sigma_e + \sigma_i + \sigma_w, \tag{5.1}$$

where σ_e is the cross section of the electromagnetic interaction, σ_w is the cross section of the weak interaction, and σ_i is the interference term of the electromagnetic and weak interactions. All the cross sections are in the c.m.s.

For ultrarelativistic electrons the cross section for weak electron-electron scattering is

$$\sigma_w = r_0^2 \left(\frac{Gm^2}{e^2}\right)^2 \left(\frac{E}{m}\right)^2 (5 + \cos^2\vartheta), \tag{5.2}$$

and the interference term has the form

$$\sigma_i = \frac{r_0^2}{\sqrt{2}} \frac{Gm^2}{e^2} \frac{5 + 3\cos^2\vartheta}{\sin^2\vartheta}, \tag{5.3}$$

where G is the weak-interaction constant, G $G = 10^{-5} M^{-2}$, and M is the nucleon mass. For the cross section of the weak annihilation $e^+ + e^- \rightarrow \mu^+ + \mu^-$ we obtain

$$\sigma_w = 2r_0^2 \left(\frac{Gm^2}{e^2}\right)^2 \left(\frac{E}{m}\right)^2 \cos^4\frac{\vartheta}{2}, \tag{5.4}$$

$$\sigma_i = \frac{1}{\sqrt{2}} r_0^2 \frac{Gm^2}{e^2} \cos^4\frac{\vartheta}{2}. \tag{5.5}$$

Comparing the energy dependence of the various cross sections, we see that with increasing energy the electromagnetic cross section decreases as E^{-2}, the interference term is independent of the energy, and the weak-interaction cross section increases, as was already noted, like E^2. It follows therefore that in the local theory the electron-electron scattering cross section has a minimum at several times 10 BeV, and that the absolute value of the cross section is very small there ($\sim 10^{-34}$ cm^2). On the other hand, if the interactions are "smeared," this minimum may not occur, and the absolute cross sections may be even smaller. At the energies attainable at the present time, the contribution of the weak interactions is rather small, for example, at 3 BeV the contribution of the weak interactions to the electron-electron scattering cross section does not exceed 0.2 per cent.

We note that if a weak interaction is realized via an intermediate boson, this leads to an appreciable distortion of the angular cross sections given above for energies exceeding the boson mass. Furthermore, if it follows from the interference term that the constant G is negative, this means that the intermediate boson does not exist.

To consider weak annihilation of an electron-positron pair into a nucleon-antinucleon pair it is necessary to take the strong interactions into account using form factors. The cross section of the process has the form

$$\sigma_w(\vartheta) = \frac{1}{2} r_0^2 \left(\frac{Gm^2}{e^2}\right)^2 \left(\frac{E}{m}\right)^2 v \left\{(F_1^2 + g_1^2)(1 + v^2\cos^2\vartheta) + \frac{M^2}{E^2}(F_1^2 - g_1^2) + 4\mu F_1 F_2 + \mu^2 F_2^2 \left[\left(\frac{E}{M}\right)^2 (1 - v^2\cos^2\vartheta) + 1\right] + 4g_1 (F_1 + \mu F_2) v\cos\vartheta\right\}, \tag{5.6}$$

$$\sigma_i(\vartheta) = \frac{1}{2\sqrt{2}} r_0^2 \frac{Gm^2}{e^2} v \left\{F_1 F_1^N \left(1 + v^2\cos^2\vartheta + \left(\frac{M}{E}\right)^2\right) + 2(\mu^N F_2^N F_1 + \mu F_2 F_1^N) + \mu\mu^N F_2 F_2^N \left[\frac{E^2}{M^2}(1 - v^2\cos^2\vartheta) + 1\right] + 2g_1 (F_1^N + \mu^N F_2^N) v\cos\vartheta\right\}; \tag{5.7}$$

Here F_1^N and F_2^N are the electromagnetic form factors of the nucleon, F_1 and F_2 are the isovector parts of the corresponding nucleon form factors, and μ^N is the anomalous magnetic moment of the nucleon, $\mu = \mu^p - \mu^n$, g_1 is the axial form factor, and v is the velocity of the produced nucleon. Near threshold σ_i amounts to 0.1 per cent of σ_e.

Along with the phenomena considered above, parity nonconservation in weak interactions will lead to characteristic polarization phenomena. The longitudinal polarization of the produced muons is given for the process $e^- + e^+ \rightarrow \mu^+ + \mu^-$ by the formula

$$P^{\pm} = \pm \varepsilon (1 + \varepsilon) \frac{(1 + \cos\vartheta)^2}{1 + \cos^2\vartheta + \varepsilon(1 + \varepsilon)(1 + \cos^2\vartheta)}, \tag{5.8}$$

where $\epsilon \approx 6.2 \times 10^{-4} (E/M)^2$.

[1] G. O'Neil, Phys. Rev. **102**, 590 (1956).

[2] V. A. Petukhov, JETP **32**, 379 (1957), Soviet Phys. JETP **5**, 317 (1957).

[3] W. Panofsky, paper at Ninth International Conference on High-Energy Physics, Kiev, 1959.

[4] W. Barber, B. Richter, W. Panofsky, G. O'Neil, B. Gittelmann, An Experiment on the Limits of Quantum Electrodynamics, Stanford, California, 1959.

[5] S. A. Kheĭfets, PTÉ, No. 6, 14 (1960).

[6] S. A. Kheĭfets, ibid, No. 6, 18 (1960).

[7] Engineer **210**, No. 5461, 519 (1960).

[8] V. S. Synakh, JETP **40**, 194 (1961), Soviet Phys. JETP **13**, 134 (1961).

[9] Data Sheets International Conference on High Energy Accelerator and Instrumentation at CERN, 1959.

[10] A. I. Akhiezer and V. B. Berestetskiĭ, Kvantovaya elektrodinamika (Quantum Electrodynamics), 2nd Ed., M., Fizmatgiz, 1959.

[11] J. Jauch, F. Rorlich, The Theory of Photons and Electrons, Cambr. Mass., 1955.

[12] M. Readhead, Pros. Roy. Soc. **A220**, 219 (1953).

[13] R. Polovin, JETP **31**, 449 (1956), Soviet Phys. JETP **4**, 385 (1957).

[14] K. Hiida, T. Murota, M. Goto, M. Sasamura, Prog. Theor. Phys., **24**, 223 (1960).

[15] H. Suura, Prog. Theor. Phys. **24**, 225 (1960).

[16] S. Tsei, Phys. Rev. **120**, 269 (1960).

[17] S. Tsei, Nuovo cimento **16**, 370 (1960).

[18] G. Rurlan, G. Peressutti, Nuovo cimento **15**, 817 (1960).

[19] G. Furlan, G. Peressutti, Nuovo cimento **19**, 830 (1961).

[20] A. A. Abrikosov, JETP 30, 96 (1956), Soviet Phys. JETP 3, 71 (1956).
[21] G.N. Garibyan, Thesis (Moscow - Erevan, 1951).
[22] V. N. Baĭer and S. A. Kheĭfets, Nucl. Phys. (1963) (in press).
[23] A. A. Abrikosov, Doctoral Thesis (Moscow, 1955).
[24] V. V. Sudakov, Candidate Thesis (Moscow, 1954).
[25] V. V. Sudakov, JETP 30, 87 (1956), Soviet Phys. JETP 3, 65 (1956).
[26] J. Schwinger, Proc. Nat. Acad. of Sci. USA 37, 452 (1951).
[27] J. Schwinger, Proc. Nat. Acad. of Sci. USA 37, 455 (1951).
[28] B. L. Ioffe, DAN SSSR 95, 761 (1954).
[29] Galinin, Ioffe, and Pomeranchuk, DAN SSSR 98, 361 (1954).
[30] E. S. Fradkin, DAN SSSR 98, 47 (1954).
[31] I. M. Gel'fand and R. Minlos, DAN SSSR 97, 209 (1954).
[32] Edwards, R. Peierls, Pros. Roy. Soc. A224, 24 (1954).
[33] I. M. Gel'fand and N. N. Chentsev, JETP 31, 1106 (1956), Soviet Phys. JETP 4, 945 (1957).
[34] V. Z. Blank, DAN SSSR 107, 383 (1956).
[35] V. Z. Blank, Candidate Thesis (Moscow, 1957).
[36] N. N. Bogolyubov and D. V. Shirkov, Vvedenie v teoriyu kvantovannykh poleĭ (Introduction to Quantum Field Theory), M., Gostekhizdat, 1957.
[37] N. N. Bogolyubov and D. V. Shirkov, DAN SSSR 103, 203 (1955).
[38] N. N. Bogolyubov and D. V. Shirkov, DAN SSSR 103, 391 (1955).
[39] N. N. Bogolyubov and D. V. Shirkov, JETP 30, 77 (1956), Soviet Phys. JETP 3, 57 (1956).
[40] N. N. Bogolyubov and D. V. Shirkov, Nuovo cimento 3, 845 (1956).
[41] D. V. Shirkov, DAN SSSR 105, 972 (1955).
[42] Landau, Abrikosov, and Khalatnikov, DAN SSSR 95, 497 (1954).
[43] Landau, Abrikosov, and Khalatnikov, DAN SSSR 95, 773 (1954).
[44] Landau, Abrikosov, and Khalatnikov, DAN SSSR 95, 1177 (1954).
[45] Landau, Abrikosov, and Khalatnikov, DAN SSSR 96, 261 (1954).
[46] A. A. Abrikosov, JETP 30, 386 (1956), Soviet Phys. JETP 3, 474 (1956).
[47] A. A. Abrikosov, JETP 30, 544 (1956), Soviet Phys. JETP 3, 379 (1956).
[48] V. N. Baĭer and S. A. Kheĭfets, JETP 40, 613 (1961), Soviet Phys. JETP 13, 428 (1961).
[49] V. N. Baĭer, Candidate Thesis (Moscow, 1960).
[50] L. Brown, R. Feynman, Phys. Rev. 85, 231 (1952).
[51] V. Z. Blank, JETP 32, 932 (1957), Soviet Phys. JETP 5, 759 (1957).
[52] K. Eriksson, A. Peterman, Phys. Rev. Letts. 5, 444 (1960).
[53] K. Eriksson, Nuovo cimento 19, 1044 (1961).
[54] L. Brown, F. Calogero, Phys. Rev. 120, 653 (1960).
[55] G. Källen, Handb. d. Phys. Bd. 5, 1958, Abt. 1.
[56] G. Chew, R. Karplus, S. Gasiorowicz, F. Zachariasen, Phys. Rev. 110, 265 (1958).
[57] W. Frazer, J. Fulko, Phys. Rev. Letts. 2, 365 (1959).
[58] W. Frazer, J. Fulko, Phys. Rev. 117, 1609 (1960).
[59] R. Hofstadter, Revs. Mod. Phys. 28, 214 (1956).
[60] R. Hofstadter, R. Herman, Phys. Rev. Letts. 6, 293 (1961).
[61] V. N. Baĭer, JETP 37, 1490 (1959), Soviet Phys. JETP 10, 1057 (1960).
[62] S. Drell, Ann. Phys. 4, 75 (1958).
[63] Berestetskiĭ, Krokhin, and Khlebnikov, JETP 30, 788 (1956), Soviet Phys. JETP 3, 761 (1956).
[64] G. Charpar et al., Phys. Rev. Letts. 6, 128 (1961).
[65] H. Fried, D. Yennie, Phys. Rev. 112, 1391 (1958).
[66] A. Zemach, Phys. Rev. 104, 1771 (1956).
[67] J. Bjorken, S. Drell, S. Frautschi, Phys. Rev. 112, 1409 (1958).
[68] I. Zlatev and P. Isaev, JETP 37, 728 (1959), Soviet Phys. JETP 10, 519 (1960).
[69] B. Richter, Phys. Rev. Letts. 1, 114 (1958).
[70] V. G. Kadyshevskiĭ, DAN SSSR 136, 70 (1961), Soviet Phys. Doklady 6, 136 (1961).
[71] V. N. Baĭer and S. A. Kheĭfets, JETP 40, 715 (1961), Soviet Phys. JETP 13, 500 (1961).
[72] A. D. Sakharov, JETP 18, 646 (1948).
[73] V. N. Baĭer and V. S. Synakh, JETP 41, 1576 (1961), Soviet Phys. JETP 14, 1122 (1961).
[74] V. N. Baĭer and V. V. Sokolov, JETP 40, 1233 (1961), Soviet Phys. JETP 13, 866 (1961).
[75] G. Furlan, Nuovo cimento 19, 840 (1961).
[76] N. Cabibbo, R. Gatto, Nuovo cimento 20, 185 (1961).
[77] J. Bowcock, W. Gottingham, D. Lurie, Phys. Rev. Letts. 5, 386 (1960).
[78] H. Wong, Phys. Rev. Letts. 5, 70 (1960).
[79] J. Anderson et al., Phys. Rev. Letts. 6, 365 (1961).
[80] N. Cabibbo, N. Gatto, Phys. Rev. Letts. 4, 313 (1960).
[81] S. Mandelstam, Phys. Rev. 112, 1344 (1958).
[82] M. Cini, S. Fubini, Ann. Phys. 3, 352 (1960).
[83] G. Chew, S. Mandelstam, Phys. Rev. 119, 467 (1960).
[84] I. Derado, Nuovo cimento 15, 853 (1960).
[85] F. Salleri, Nuovo cimento 16, 775 (1960).
[86] P. Carruthers, H. Bethe, Phys. Rev. Letts. 5, 161, (1960).
[87] E. Pickup et al., Phys. Rev. Letts. 6, 161 (1961).
[88] L. Afrikyan and G. Garibyan, JETP 33, 425 (1957), Soviet Phys. JETP 6, 331 (1958).
[89] R. Carplus, C. Sommerfeld, E. Wichman, Phys. Rev. 111, 1187 (1959).
[90] Y. Nambu, Phys. Rev. 106, 1366 (1957).

[91] V. B. Berestetskiĭ and I. Ya. Pomeranchuk, Nucl. Phys. **22**, 629 (1961).
[92] R. Feynman, M. Gell-Mann, Phys. Rev. **109**, 193 (1958).
[93] S. Bludman, Nuovo cimento **9**, 433 (1958).
[94] V. N. Baĭer and I. B. Khriplovich, JETP **39**, 1374 (1960), Soviet Phys. JETP **12**, 959 (1961).
[95] C. Bernardini et al., Nuovo cimento **23**, 202 (1962).
[96] B. Touschek, International Conference on Theoretical Aspects of Very High Energy Phenomena, CERN, 1961.
[97] S. A. Kheĭfets, Lecture at the School of Physics in Nor-Amberd, Proc. of the 2nd Session of the School of Physics in Nor-Amberd, Erevan, 1962.
[98] V. N. Baĭer and S. A. Kheĭfets, paper at the III Uzhgorod Conference. Proc. of the III All-Union Uzhgorod Conference, Uzhgorod, 1961.
[99] I. Harris, L. Brown, Phys. Rev. **105**, 1656 (1957).
[100] G. Andreassi, P. Budini, G. Furlan, Phys. Rev. Letts. 8, 184 (1962).
[101] A. Layzer, J. Math, Phys. **2**, 308 (1961).
[102] B. Maglic, et al., Phys. Rev. Letts, 7, 178 (1961).
[103] D. Stonehill et al., Phys. Rev. Letts. **6**, 624 (1961).
[104] R. Barloutaud et al., Phys. Rev. Letts. 8, 32 (1962).
[105] S. Fubini, Phys. Rev. Letts. 7, 466 (1961).
[106] P. Bastiene et al., Phys. Rev. Letts. 8, 114 (1962).
[107] M. Gell-Mann, D. Sharp, W. Wagner, Phys. Rev. Letts. 8, 261 (1962).
[108] N. Cabibbo, R. Gatto, Phys. Rev. **124**, 1577 (1961).
[109] V. N. Gribov and I. Ya. Pomeranchuk, JETP **42**, 1141 (1962), Soviet Phys. JETP **15**, 788 (1962).

Translated by A. M. Bincer and J. G. Adashko